ThalesAlenia
Space
A Thales / Finmeccanica Company

AHEAD 2020

Funded by the Horizon 2020 Framework
Programme of the European Union
Grant Agreement No. 871158

SRON — Netherlands Institute for Space Research

INFN — Istituto Nazionale di Fisica Nucleare

UNIVERSITÀ DEGLI STUDI DI GENOVA

KAON — VACUUM & CRYOGENICS

INAF — ISTITUTO NAZIONALE DI ASTROFISICA

WP15 Deliverable D15.6

Detailed design requirements
of the TES spectrometer

Project acronym:
AHEAD2020

Project Title: **Integrated Activities for the High Energy Astrophysics Domain**

Grant Agreement No: **871158**
This deliverable is part of a project that has received funding from the European Union's Horizon 2020 research and innovation programme

Start date of the project:
2020-03-02

Written by	*Responsibility* + handwritten signature if no electronic workflow tool
P. Bastia (TAS-I) M. Chiari (INFN/LABEC) F. Gatti (UniGe) P. Khosropanah (SRON) U. Lo Cicero (INAF/OAPA) K. Phelan (Kaon Gmbh)	WP15 tasks coordinators
Verified by	
P. Bastia	WP 15 leader
Approved by	
L. Natalucci	AHEAD2020 Project Scientist

Approval evidence is kept within the documentation management system.

OPEN

CHANGE RECORDS

ISSUE	DATE	§ CHANGE RECORDS	AUTHOR
1	Aug 2021	Version for final revision	All tasks coordinators

TABLE OF CONTENTS

OPEN

OPEN

1. SUBJECT

This document reports the set of requirements for the design and construction of the TES X-ray spectrometer prototype to be realized in the frame of the AHEAD2020 project WP15.

These requirements have been identified, discussed and agreed by the WP15 partecipants during a series of meeting from the project start.

For the main scientific requirements a verification method is proposed within this document to provide a guide for the test and integration phase.

The document also shows some design implementation details with the purpose of better describe what the requirements are aimed to.

1.1 Structure of the document

This document is structured as follows:

Chapter 3   gives an introduction to the AHEAD2020 project

Chapter 4   gives an high-level view of the spectrometer prototype

Chapter 5   gives the full set of requirements and the implementation baseline

OPEN
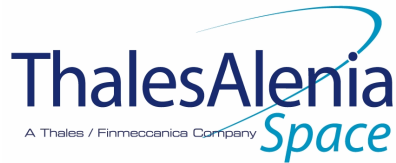
1.2 Acronyms list

ADC	Analog to Digital Converter
ADR	Adiabatic Demagnetization Refrigerator
AHEAD	integrated Activities for the High Energy Astrophysics Domain
AIV	Assembly Integration and Verification
CFEE	Cold Front End Electronics
DAC	Digital to Analog Converter
DR	Dynamic Range
EC	European Commission
ESA	European Space Agency
ETF	Electro Thermal Feedback
EU	European Union
FEE	Front-End Electronics
FDM	Frequency Division Multiplexing
FWHM	Full Width at Half Maximum
FLL	Flux Locked Loop
FOV	Field Of View
ICD	Interface Control Document
LNA	Low Noise Amplifier
MIP	Minimum Ionizing Particle
PCB	Printed Circuit Board
PIXE	Particle Induced X-ray Emission
P/L	Payload
QE	Quantum Efficiency
SQUID	Superconducting Quantum Interference Device
SRON	Space Research Organization of Nederland
SpW	SpaceWire
TAS	Thales Alenia Space
TAS-I	Thales Alenia Space-Italia
TBC	To Be Confirmed
TBD	To Be Defined
TBV	To Be Verified
TBW	To Be Written
TES	Transition Edge Superconductor
TDM	Time Division Multiplexing
TM/TC	TeleMetry and TeleCommand
WBEE	Warm Back End Electronics
WFEE	Warm Front End Electronics
WP	Work Package

OPEN

2. APPLICABLE AND REFERENCE DOCUMENTS

2.1 Applicable Documents

AD1:   Grant Agreement number: 871158 — AHEAD2020
            H2020-INFRAIA-2018-2020/H2020-INFRAIA-2019-1

2.2 Reference Documents

RD1:   Internal minute of meeting #1, issued May 20, 2020
            MOM15.2_1

RD2:   Internal minute of meeting #2, issued June 11, 2020
            MOM15.2_2

RD3:   Internal minute of meeting #3, issued July 07, 2020
            MOM15.2_3

RD4:   Internal minute of meeting #4, issued Aug 04, 2020
            MOM15.2_4

RD4bis: Short Form MOM of telecon held October 14, 2020
            attached to mail the same day

RD5:   Internal minute of meeting #5, issued Oct 28, 2020
            MOM15.2_5

RD6:   Internal minute of meeting #6, issued Nov 14, 2020
            MOM15.2_6

RD7:   Internal minute of meeting #7, issued Feb 08, 2021
            MOM15.2_7

RD8:   Internal minute of meeting #8, issued Mar 16, 2021
            MOM15.2_8

RD9:   Internal minute of meeting #9, issued April 13, 2021
            MOM15.2_9

RD10:   Internal minute of meeting #10, issued July 21, 2021
            MOM15.2_10,

OPEN

RD11: P. Peille & al. "Quantifying the effect of cosmic ray showers on the X-IFU energy resolution", poster presented at LTD-18, Milan. July 22-26, 2019

RD12: Data provided by SRON during discussion (mail from P. Khosropanah, October 15, 2020).

RD13: P.D. Mauskopf et al. "A TES Focal Plane for SPICA-SAFARI" 21ST INTERNATIONAL SYMPOSIUM ON SPACE TERAHERTZ TECHNOLOGY, OXFORD, 23-25 MARCH, 2010

3. INTRODUCTION

AHEAD2020 (integrated Activities for the High Energy Astrophysics Domain) is a collaborative research project carried on by a consortium of 38 institutions from 16 countries within the Horizon 2020 initiative funded by the EU.

The AHEAD2020 overall objective is to advance the integration of national efforts in high-energy astrophysics, keeping the community at the cutting edge of science and technology and ensuring that observatories are at the state of the art.

The AHEAD2020 project also aims to further integrate activities with the recently born multimessenger astronomy, boosted very recently by the discovery of gravitational waves and cosmic neutrinos and of their first high energy counterparts. This is achieved by a large community of high energy astronomers, gravitational wave and astroparticle scientists.

Technological developments within the project will focus on the improvement of selected detector, optics devices and advanced analysis tools for the benefit of future space missions and ground-based multimessenger facilities, with more emphasis on the observation of the new transient Universe.

Furthermore AHEAD2020 integrates key infrastructures for on-ground test and calibration of space-based instrumentation and promote their coordinated use.

The AHEAD2020 project also includes a dedicated work package (WP15) devoted to technology innovation with the aim to explore the transfer of technologies developed in the AHEAD2020 project to other applications relevant to the high-tech industrial market, both in the space domain and for "ground" applications. One of the main tasks (WP15.2) is the development of a prototype X-ray spectrometer system based on TES detector to be used in science laboratories on ground, with focus on the PIXE (Particle Induced X-ray Emission) technique applied to environmental analysis and cultural heritage studies.

OPEN

In this document we identify a comprehensive set of requirements for the X-ray spectrometer systems based on TES detector to be realized within task 15.2. These requirements will constitute the basis for the implementation phase of the system.

4. HIGH-LEVEL DESCRIPTION OF THE X-RAY SPECTROMETER SYSTEM

The project task is to develop a prototype of a compact TES X-ray spectrometer to be used in a PIXE facility for measurements requiring high energy resolution.
The baseline is to use a small ADR-based cryostat (from Kaon GmbH) with a protruding snout (PROBE) hosting the detector at its tip.

As a preliminary scenario we assume that the spectrometer system should have a general structure as shown in the sketch in Fig. 4.1.
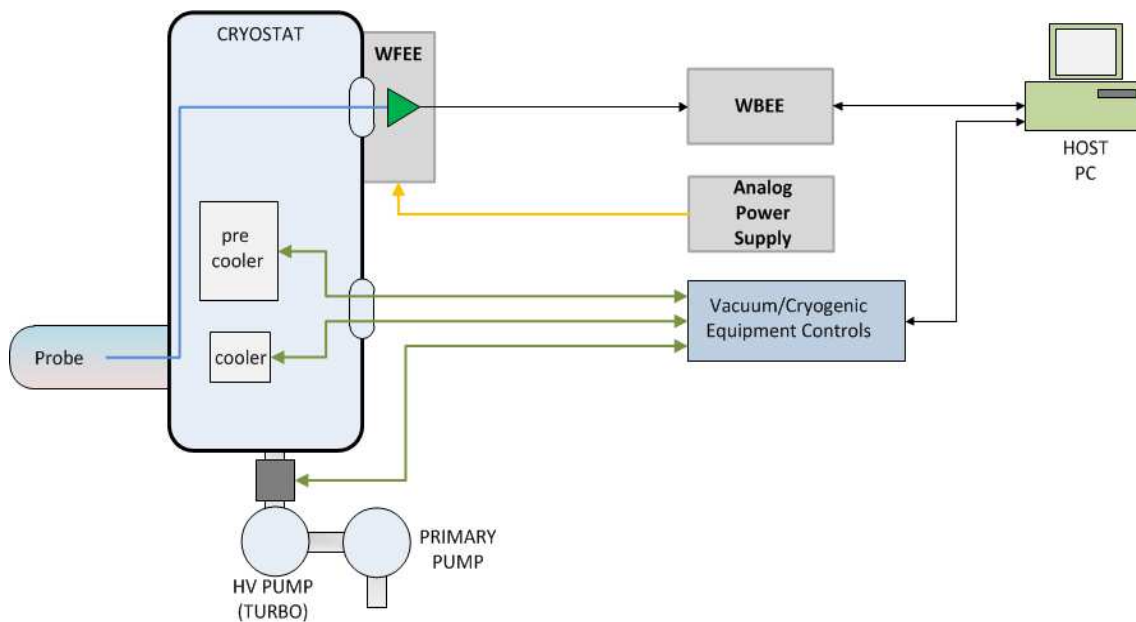
Fig. 4.1 sketch of the TES spectrometer prototype to be developed in WP 15.2

The main elements of the system are:

1) a compact cryostat including a pre-cooler chain to provide ~0.5 W of cooling power to a flange held at ~4 K, and a final ADR cooler stage providing cooling power of ~1μW down to a base temperature of 50 mK for TES operation with a transition temperature around 100 mK. In the envisaged configuration the TES detector shall be installed close to the

OPEN

top of a "snout" probe which protrudes from the cryostat main vessel to allow close proximity with the target.

2) The snout probe should be flange-mounted to the cryostat vessel so to share the same vacuum environment. The probe shall include an inner cold-finger thermally connected to the cold stage to provide enough cooling power for the TES operation. A removable Detector Holder on top of the cold-finger will support the detector chip and the related chipset up to the FE SQUID (preamplifier) and the related cryo-harness routing to a connector for the readout. Shrouds at intermediate cryogenic temperatures (baseline at 4 K and 70 K) should be provided to reduce the heat load on the cold finger from the probe walls.

3) A secondary cold finger at T=1 K (nominal) is foreseen to host the AMP SQUID, possibly with local shroud and magnetic shield.

4) An entrance window and a set of thermal/optical filters are to be provided in the probe to allow x-ray transmission while blocking thermal radiation, which would degrade the TES performances.

5) Magnetic shielding should be provided at least immediately around the detector to reduce the effect of stray and ambient magnetic fields on the detector performance.

6) A cryo-harness for the routing of signals and biases from/to the detector is a critical matter as it implies a thermally conductive path toward the 50-100 mK environment that should be minimized to stay with reasonable cooling power requirements for this stage. The cryo-harness should be heat-sinked (thermal clamps) at various temperature stages from room temperature to the cold finger.

7) Readout Electronics: these shall be composed by a Warm Front End Electronics (WFEE) and a Warm Back End Electronics (WBEE) and a Host PC to allow an easy human interface to set the instrument and collect data. In the frame of the AHEAD2020 project the detector shall be an array of few tens of TES and the envisaged multiplexing solution is the Frequency Division Multiplexing (FDM) approach as developed by SRON. In short the FDM approach foresee that the TES array biased in parallel by the same bias line providing a "comb" of AC carriers in the MHz range. Each TES is connected to the common bias line via a high-Q resonant filter so that it only responds to a given carrier frequency: the useful signal is the amplitude of the current flowing in the TES at that frequency. All the TES are then connected to a single SQUID which add all their signals and provides their amplification and routing to the warm electronics where the individual TES signal amplitudes can be reconstructed by demodulation of each individual frequency.

8) Ancillary equipment: these will be set of devices, mainly procured off the shelf, as follows:

OPEN

- vacuum gauges, at least a vacuum and a high-vacuum gauges to provide monitoring and logging of the vacuum environment and to provide alarms in case of leakages.
- turbo-pump controller to manage the turbo pump (start-up, running, shut down cycles)
- controls electronics for the various cryocoolers stages (e.g. pulse tube, ADR)
- temperature control and logging
- host PC

The set-up of the cryostat section (i.e. not including the probe and the spectrometer readout electronics) will be composed by the cryostat itself mounted on a movable support including the vacuum pumps plus a mini-rack hosting the ancillary equipment and a host PC.

The cryostat body includes a set of shrouds to limit thermal radiative transfer between the cooler stages and the environment.

The cryostat top flange hosts a suitable number of ports (plus a vent valve) for connection to the vacuum system and for different electrical connections which should be divided in the following classes:

- power lines to the coolers
- control lines to the coolers
- temperature monitoring network
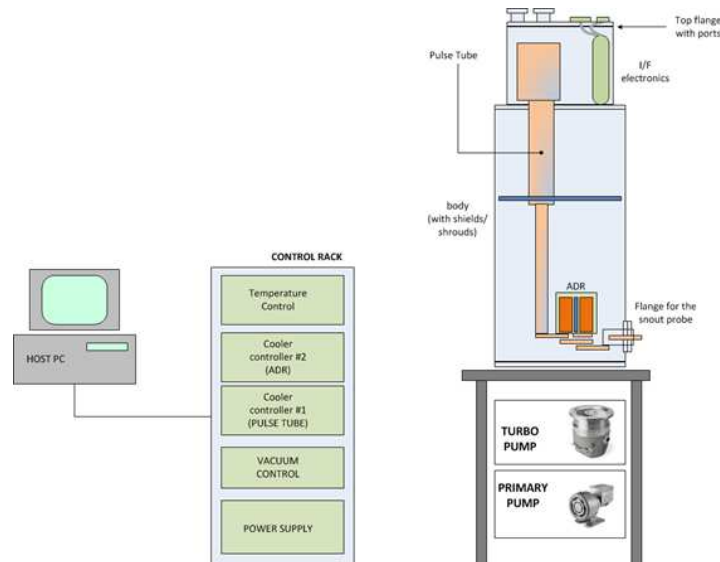- instrument-related connections (depending on the WFEE implementation)

Fig. 4.2: sketch of a possible cryostat section set-up
(not including the spectrometer-related HW)

OPEN

4.1 Scientific performance requirements

The target performances for the envisaged PIXE application are as follows:

Energy range: 1-10 keV

Energy resolution: < 15 eV FWHM @ 5.9 keV

Count Rate: > 1 ksps overall, to be traded with other parameters

FOV: > 0.3 msr (milli-steradians)

4.1.1 Scientific performance requirements verification

These performances will be verified during the AIV phase of the spectrometer prototype by means of low-intensity radioisotope calibration sources.

The energy range requirement will be verified using a set of (few) known calibration sources with discrete energies covering the required range.
The set up will provide a low overall count rate to minimize pile-up effects.
The count rate of each pixel of the array will be measured and compared with the expected count rate expected from the source calibrated activity and the geometrical set up.

The energy resolution requirement will be verified stimulating the fully integrated spectrometer with a Fe55 calibration source illuminating the whole array with an exposure time in the order of 3600 sec.

The count rate requirement will be verified gradually increasing the photon rate (acting on the source-detector set-up geometry) to characterize the pile-up effect from which the count rate limits could be derived.

The FOV requirement will be verified by analysis (geometry); it will be cross-checked during the above described test in terms of respondence between expected and measured counts.

4.2 Mechanical/Electrical/Cooling requirements

The mechanical/thermal guideline requirements to start from are given herebelow, we assume the system should stay in these mass/dimension/power budget (cryostat + ancillary equipment).

Mass:	< 500 kg
Volume:	< 3 m³
Area:	< 3 m²
Power:	< 7 kW, 400 V, 1 kW 230 V
Water (cooling loop):	< 10 l/min @ 10-20°C

4.3 PROBE prototype concept

The detector and the related chipset for FDM readout will be provided by SRON, the proposed set of devices is as follows (data summary, see relevant chapter for details on each device):

- Detector chip, 8 x 8 = 64 pixels of which only 32 will be used in the prototype readout.

- LC-filter chip,

- 1st stage SQUID (FE SQUID)

Note: the selected detectors can be directly coupled with the related LC-filters without need for a coupling transformer.

These devices will be mounted onto the Detector Holder platform, a removable device which is installed on the cold-finger top and thermally connected to it.

The envisaged base temperature for the cold-finger (Detector Holder) is 50 mK (with no load).

The detector transition is close to 100 mK

The power dissipation at 100 mK will be < 1µW for the whole chipset.

A second stage SQUID (AMP SQUID) is also foreseen at 1 K secondary cold finger with < 1 µW power dissipation used to drive the signal from the probe up to the room temperature flange. The following figure gives a visual description of the above elements.

OPEN
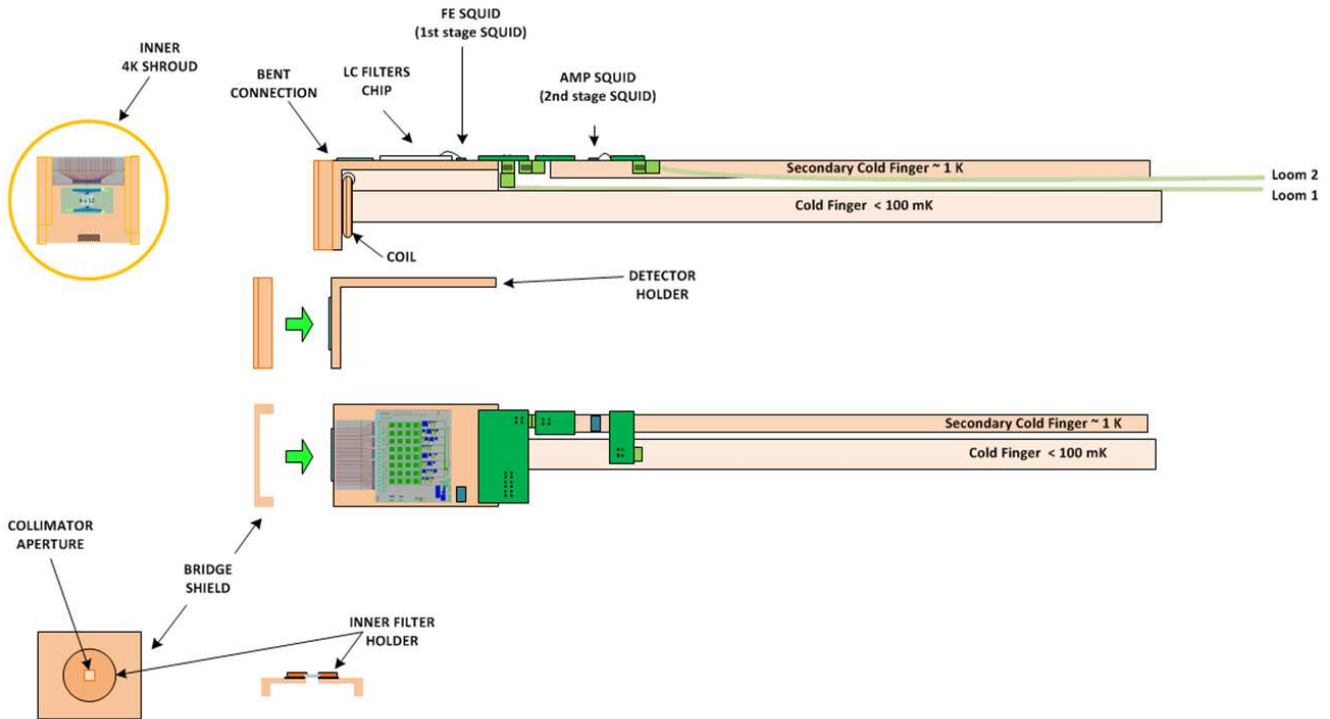
Fig. 4.3.1: sketch of the Detector Holder, Cold Finger, Secondary Cold Finger
(only conceptual not truly representative nor to scale w.r.t the actual design)

A dedicated "bent connection" made by superconductive flex cable is foreseen to connect the detector chip with the LC-filter chip at 90° relative orientation.

A so-called "bridge" shield is foreseen in front of the detector to provide a local 100mK shroud and to host the inner optical filter.

Fig. 4.3.2: bent connection prototype design

OPEN

4.4 Probe operating scenario

The probe will operate close to the output of the P+ beamline at the tandem proton accelerator at INFN LABEC laboratory in Florence. The targeted PIXE experiments takes place in air where the target is placed at few cm from the beamline output window. A flux of gaseous He is also used in some cases to minimize X-ray absorption from air, this may better be conveyed using a containing cap surrounding the volume in front of the entrance window.
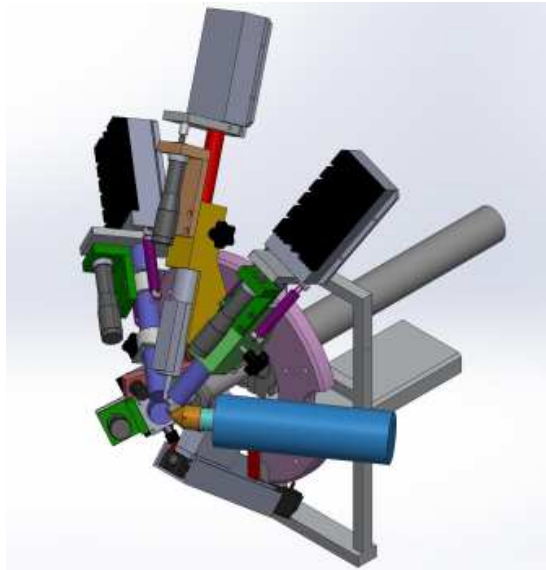
Fig. 4.4.1: Experimental arrangement at the LABEC beamline, the allocated volume for the TES probe is the blue cylinder which in this rendering is 200 mm long and 60 mm diameter

The operating area is quite cramped and for this reason the probe should be designed to have a small volume in proximity of the target and a protruding or "snout" layout is envisaged.

The envisaged appearance of the spectrometer is as follows:

OPEN
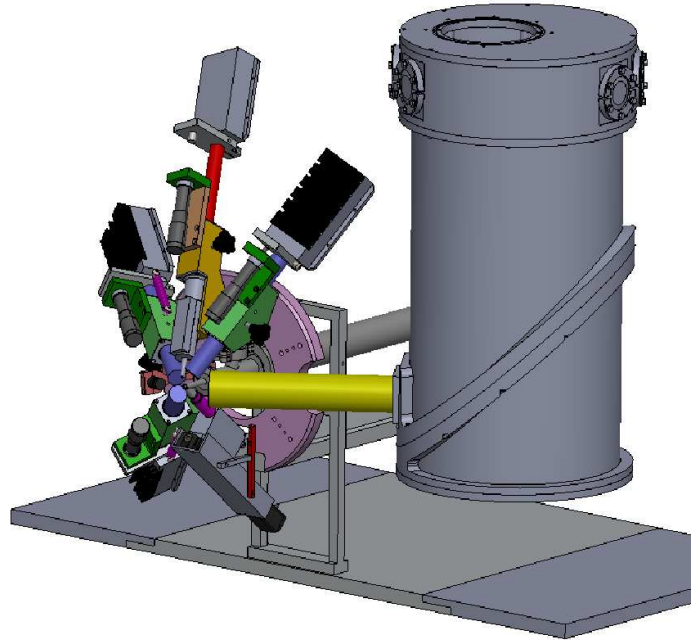
Fig. 4.4.2: Sketch of the spectrometer snout probe and cryostat case
(ancillary equipment not shown)
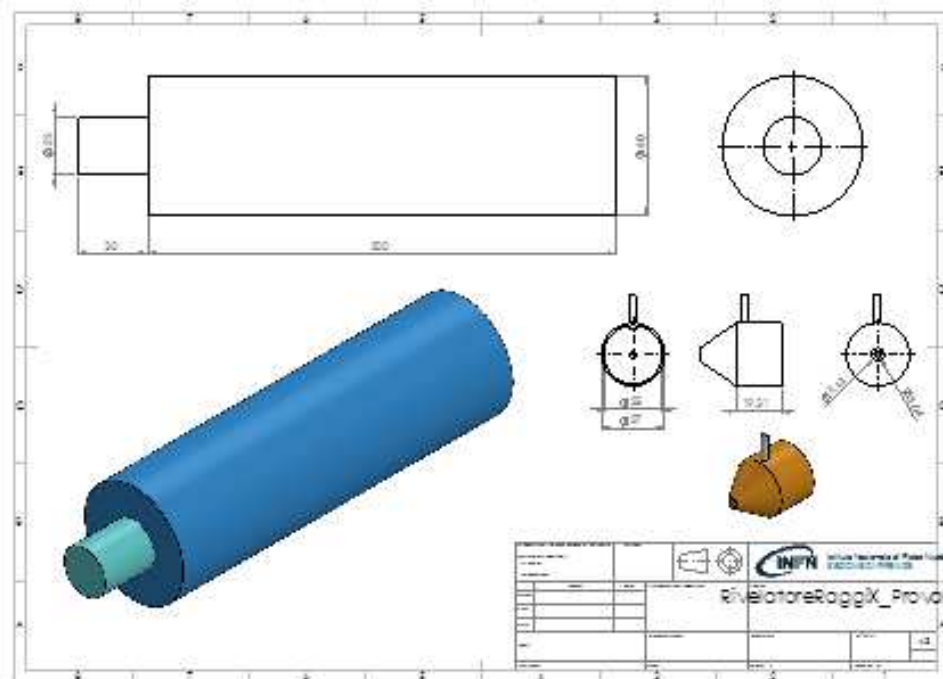
Fig. 4.4.3: Snout probe available volume. The orange cap is for He fluxing when needed

OPEN

5. DETAILED REQUIREMENTS

This chapter reports the detailed requirement for each element of the X-ray spectrometer system object of WP15.2 as agreed by the relevant task leader.

5.1 SNOUT probe requirements

5.1.1 Geometry and dimensional limits:

The set of requirements identified so far for the snout are given in the following table:

Shape: cylindrical
Diameter: ≤ 60   mm
Length: ≥ 200 mm

5.1.2 Photon collection geometry (FOV):

This is dependent on the distance between the target (proton impinging area, assumed point-like) and the detector and also on the detector area. The overall experimental arrangement is conditioned by the beamline exit pipe having a diameter of 8 mm and by the diameter of the snout probe, possibly taking in account a degree of tapering at the snout front side.

The following figure shows a sketch of a typical arrangement with a snout having 48 mm diameter with no tapering.

OPEN
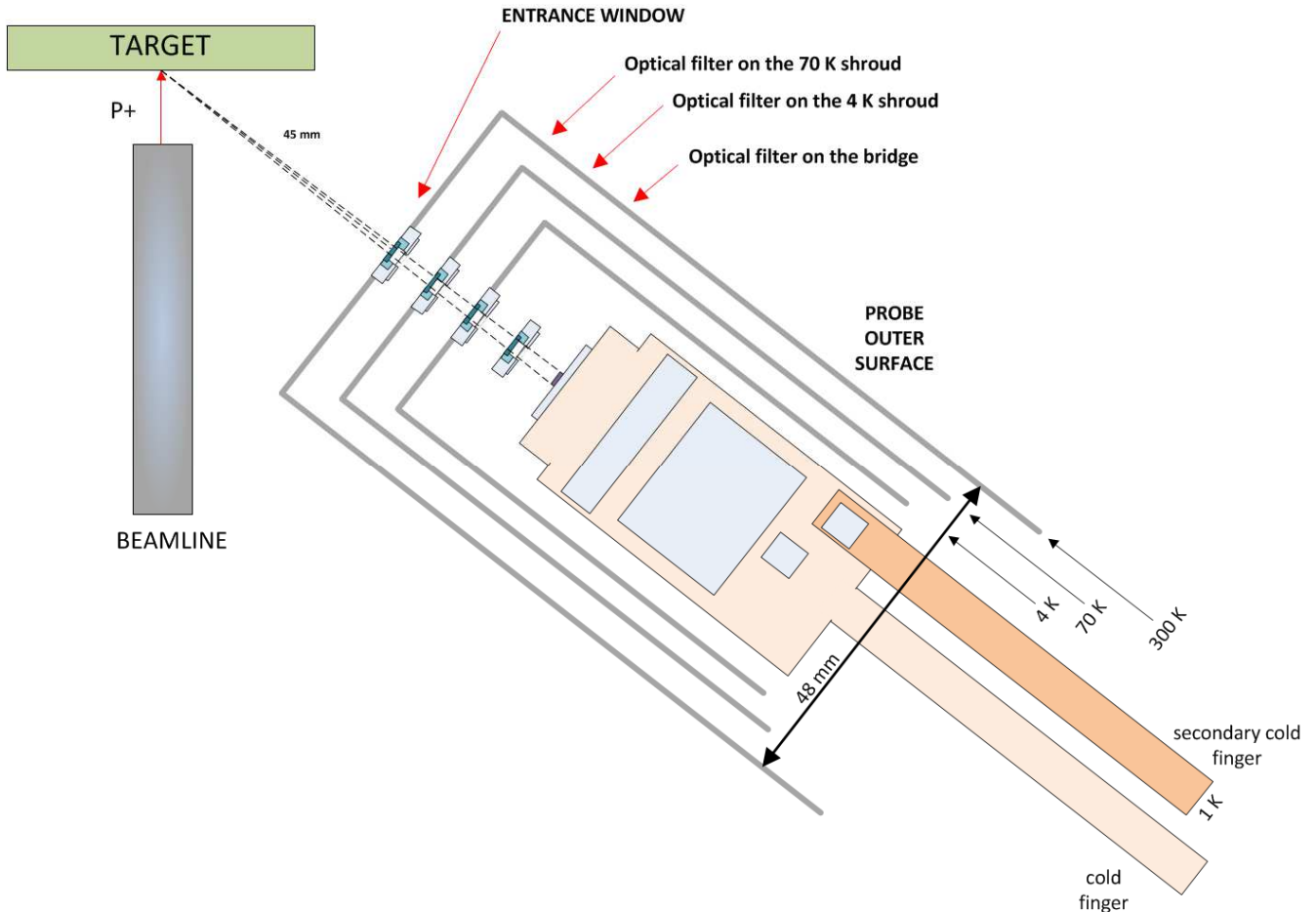
Fig. 5.1.2.1: sketch of a probe-target arrangement (concept only)

The above sketch (very crude) takes in account the latest design evolution in terms of probe diameter and number of shrouds etc. and would result in a detector-target distance of ~ 74 mm Which would give a solid angle around 0.33 msr, (assume 32 pixel 0.24 x 0.24 mm² each).

This value would be in agreement (but close to the limit) to the required 0.3 msr, some trading still being possible between the snout external diameter, the inter-distance between the different shrouds (and related optical filters) and the tapering angle.

Note the above estimation includes a 45 mm minimum distance between the target and the entrance window which is a limit imposed by the current LABEC set-up. The strictly geometrical constraints of the probe would allow a factor ~2 improvement.

5.1.3 Probe external and inner architecture:
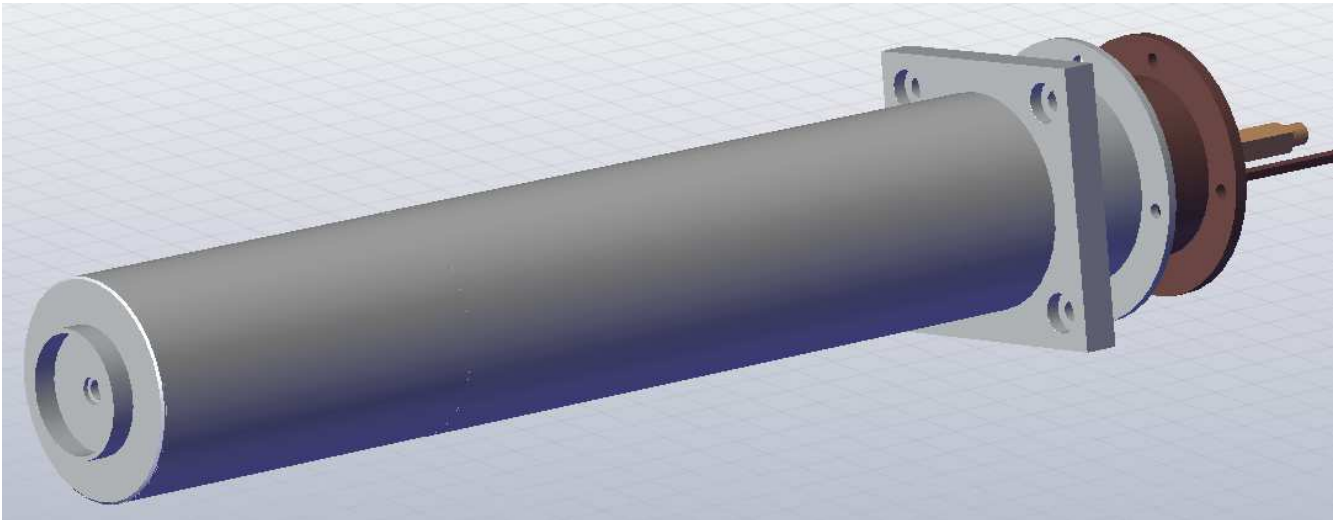
Fig, 5.1.3.1: External view of the snout

As shown in the above figure the prototype snout has a cylindrical shape with a flat front face.
A rim around the entrance windows is foreseen to protect the entrance window and to allow mounting of accessories like e.g. a cone to confine helium when working with He flux.

The design of the snout foresee that the every part of the front section can be removed so to have an easy access to the detector holder volume for maintenance and checkout.

A few views of the internal structure are given here below:
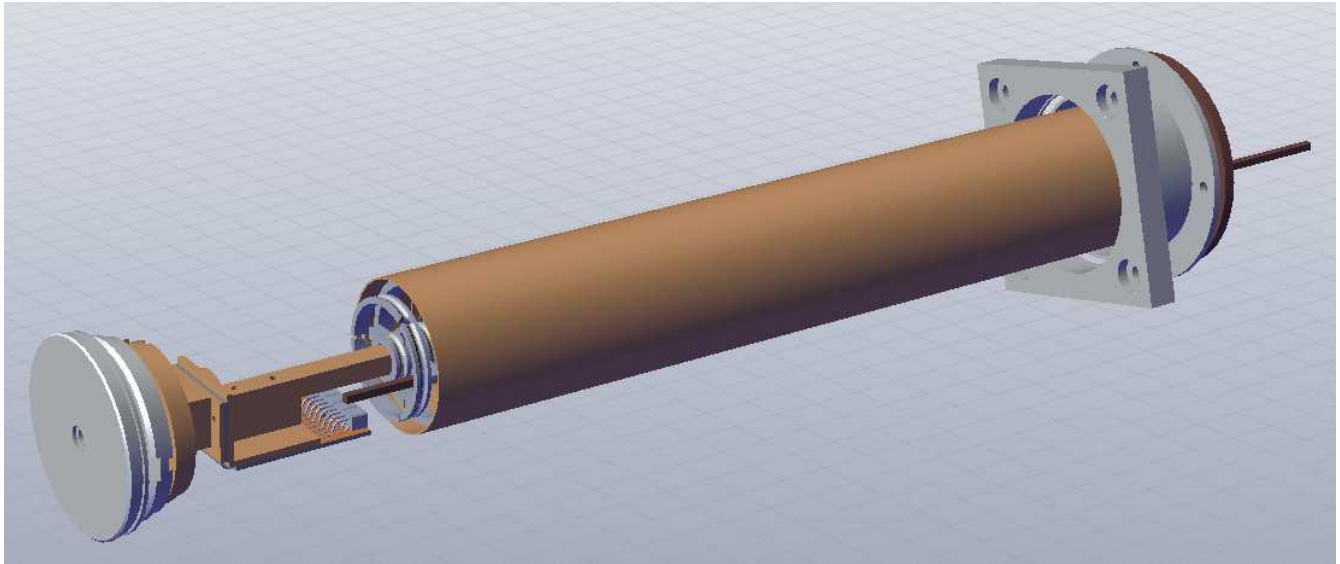
Fig, 5.1.3.2: internal view of the snout showing the 4 K shroud with front sections removed
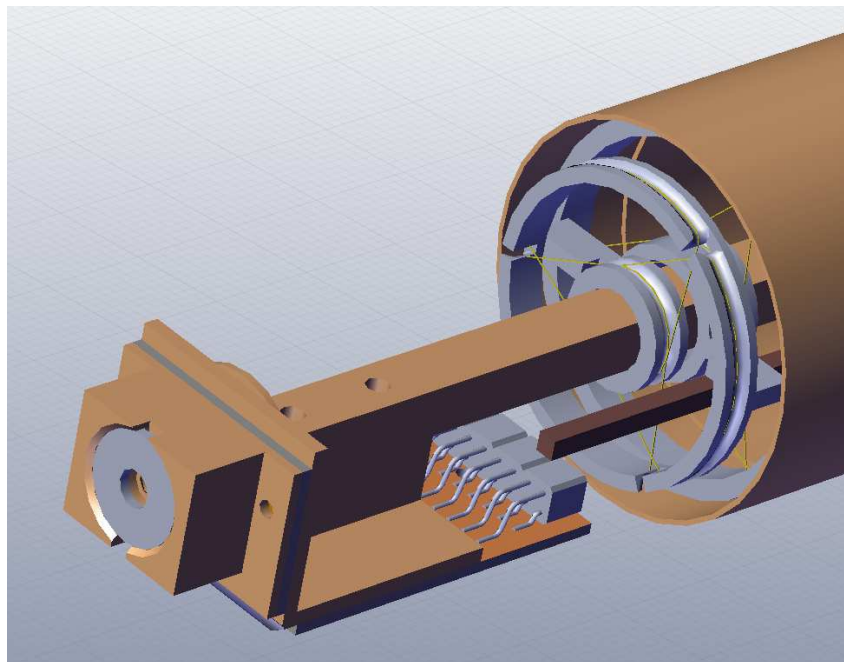
Fig. 5.1.3.3: detail of the Detector Holder and the "bridge"

OPEN
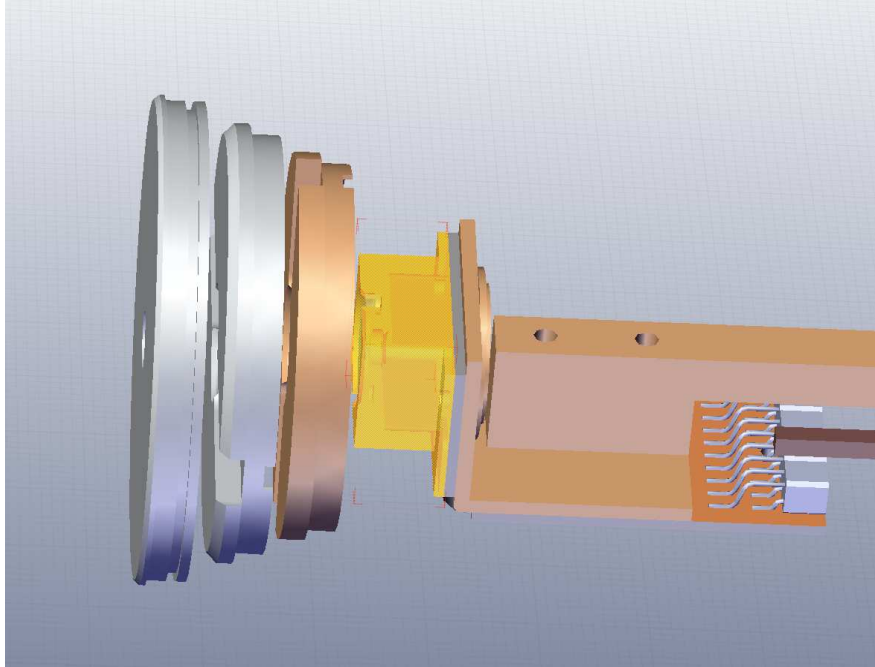
Fig. 5.1.3.4: view of the front cap and inner caps arrangement

5.1.4 Nominal temperatures of the snout elements:

Cold finger nominal temperature: 50 mK @ no load

"Bridge" structure surrounding the detector:
nominal temperature: < 100 mK
detector-ceiling distance   5 mm
bridge mounting: screwed on the detector holder
Optical function: hosts the Inner optical filter and aperture

Coaxial shrouds surrounding the cold finger:
Inner shroud nominal temperature: 4 K
Inner shroud radius: TBD, depends on the detector dimensions
Inner shroud mounting: flange mount on the 4 K cooler stage
Optical function: hosts the 4 K optical filter and aperture

Intermediate shroud nominal temperature: 70 K
Intermediate shroud radius: TBD, depends on the detector dimensions
Intermediate shroud mounting: flange mount on the 70 K cooler stage
Optical function: hosts the 70 K optical filter and aperture

OPEN

Vacuum wall:
Nominal temperature: 300 K
Vacuum wall radius: < 60.0 mm (general requirement)
Vacuum wall mounting   flange mount on the cryostat vessel
Optical function: hosting entr. window (pressure resistant)

The detector and its chip set shall be mounted on a thermally conductive structure known as Detector Holder providing a mechanical and thermal interface to the cold finger. The Detector Holder shall provide the necessary electrical interface to the harness via a connector to allow an easy removal for maintenance or modification /substitution.

The cold finger shall be mechanically suspended to the 4 K shroud to maintain the axial detector position, a solution presently pursued is to have it suspended by a net of aramid wires so allowing a small degree of axial displacement to account for thermal contraction during cooldown.

A secondary cold finger at nominal 1 K is foreseen to host the AMP SQUID on a dedicated platform close to the Detector Holder
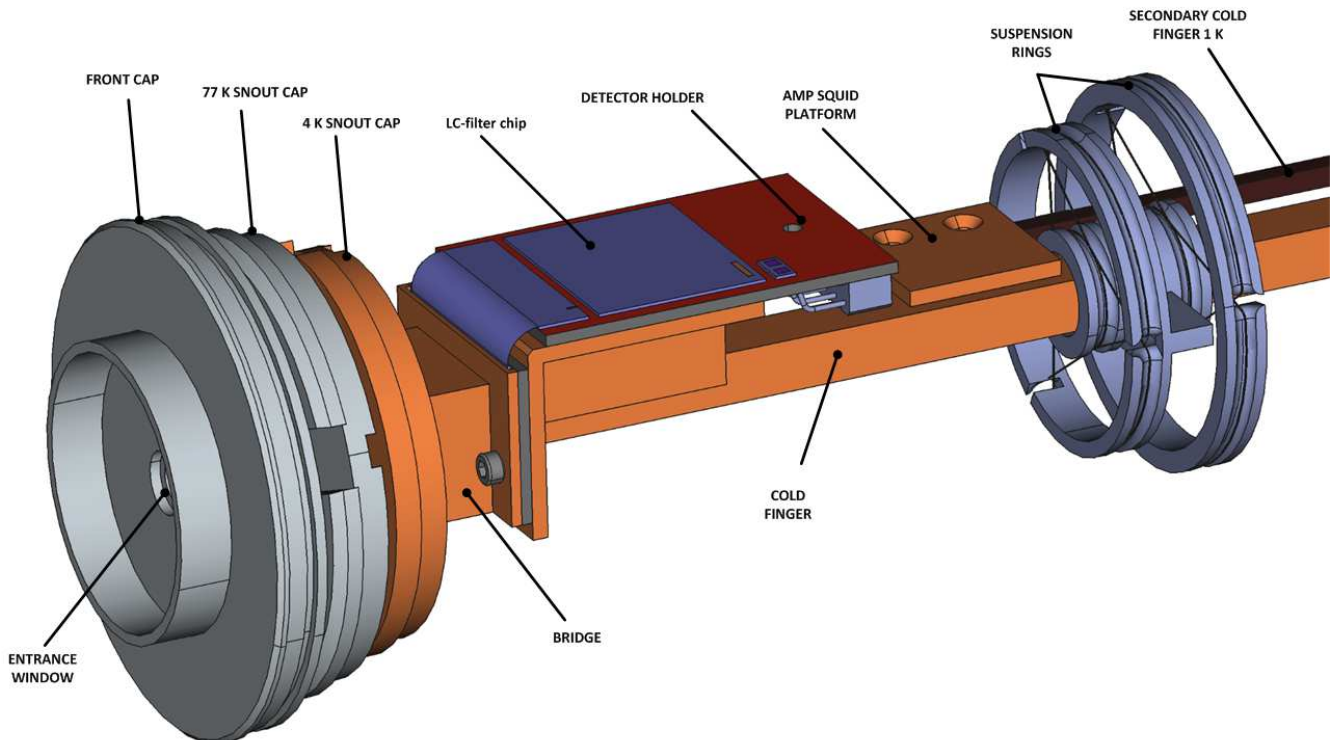
Fig. 5.1.4.1: rendering of the main components of the snout with nomenclature

OPEN

5.2   Detectors requirements

Detector type: pixellated TES detector optimized for 1-10 eV X-ray spectroscopy
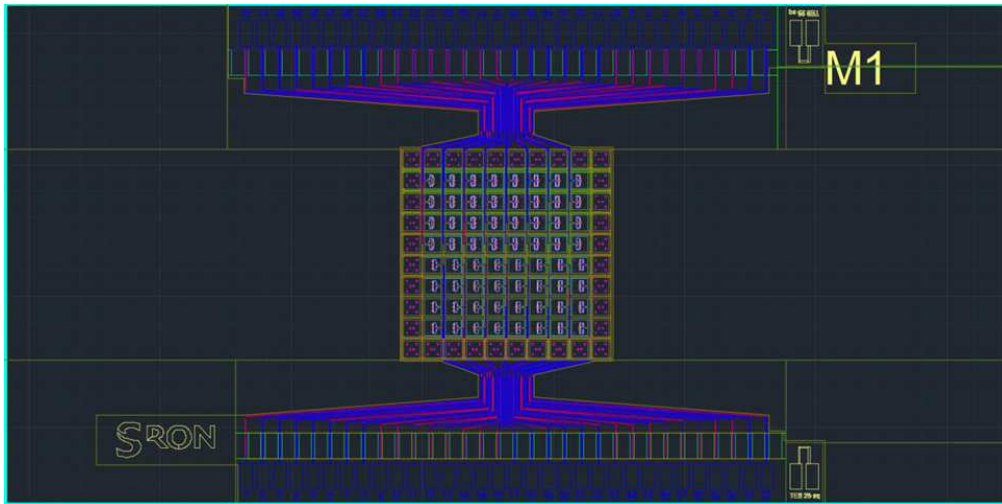
Fig. 5.2.1: detector chip layout

Chip dimensions: 6 x 12 mm²

Pixel size: 240 µm side
Pixel array organization: 8 x 8 square array, 32 usable in prototype, 250 µm pitch
Absorber thickness: 2.3 µm (material: Au)

Rnormal: 90 to120 mohm
R operating point: 18 to 40 mohm

Biasing scheme: shunted bias current, Rshunt = 0.75 to 1 ohm
Bias at operating point: typ 10 µA

Power dissipation: typ 100 pW (32 pixel)

T transition: typ 90 mK +/- 1 mK across the array

Si Substrate thickness: 300 µm

SiN membrane thickness: 500 nm

5.2.1 Superconductive transformers

NOT USED WITH THE SELECTED CHIPSET

5.2.2 Frequency selection filters
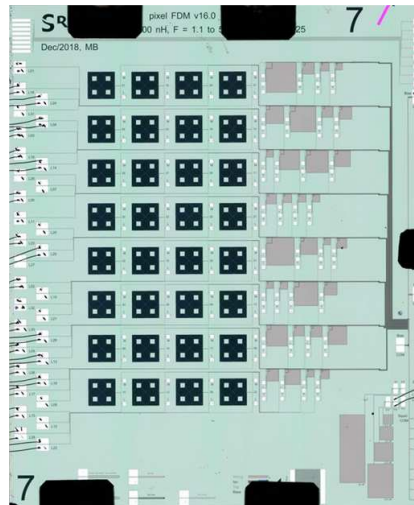
Fig. 5.2.2.1: L-C filters chip layout

Chip dimensions: 20.0 x 16.5 mm²

Organization: 32 channels, in a 4 x 8 array (see Fig. 5.2.2)

Resonance frequencies: 1 to 5 MHz (100 kHz spacing)
                          L = 2 µH for all channels

Note: each resonator consists of 2 capacitors (Cbias and Cmain) that is basically a voltage divider. In the current baseline Cmain/Cbias=25 to reduce the bias voltage across the device by a factor of 25.

Operating T: typ 50 mK

Power dissipation: Negligible

5.2.3 SQUID stages

5.2.3.1   FE SQUID stage:

Chip dimensions: 4 x 2 mm²

Organization: 1 squid device with input and output coil

Operating T: typ 50 mK

Biasing scheme: shunted, Rshunt ~ 1 ohm

Power dissipation: typ. 2 nW

5.2.3.2   AMP SQUID stage:

Chip dimensions: 4 x 4 mm²

Organization: 1 squid device with input and output coil

Operating T: typ. 1-2 K

Biasing scheme: shunted, Rshunt ~ 1 ohm

Power dissipation: typ. 1 µW

5.3   Optical / Thermal filters requirements

The TES detectors envisaged in this type of applications are very sensitive to disturbances so that any care must be taken to avoid out-of-band radiation to impinge on the focal plane.

For this reason, the cold-head assembly shall be built with materials that can work also as a radiation shield from all not-FOV directions (including magnetic shields as described in next chapter), while for the needed FOV windows a set of optical and thermal filters is to be provided.

The design of these filters is a non-trivial task as they shall be at the same time transparent to the radiation to be detected, to keep a good overall Quantum Efficiency of the detector, while opaque to all out-of-band components, to avoid a degradation of the energy resolution due to photon shot noise.

In the case of a **soft x-ray** detector the filters shall be transparent enough to let trough ~ 1 keV soft x-ray photons while minimising visible, UV or IR contributions.

OPEN

A distributed filtering optimizes the compromise between thermal radiation shielding capabilities and X-ray transparency, thus a filter is foreseen at each stage of the cryogenic system: an external window mounted on the external cap and three internal filters mounted respectively on the 70 K snout cap, on the 4 K snout cap and on the mK bridge. The temperature of the bridge and the coolest filter needs to be close to the temperature of the detector to avoid an unfiltered radiating load.

In terms of X-ray transparency, the filter stack can be viewed as a single filter composed by the sum of the thicknesses of the various filter materials. In order to evaluate the photon shot noise generated onto the detector a more sophisticated analysis is required, that includes the effects of the system geometry and the multiple reflections of the IR photons. To minimize the thermal contribution due to the multiple reflections, and in general to limit the photon flux toward the detector, the filter diameter has to be kept as low as possible. Mounting the filters with a small tilt with respect to the detector plane, may help in further reducing the multiple reflections contribution.

As a baseline scheme for the TES spectrometer prototype, we foresee a scheme as shown in Fig 5.3.1.
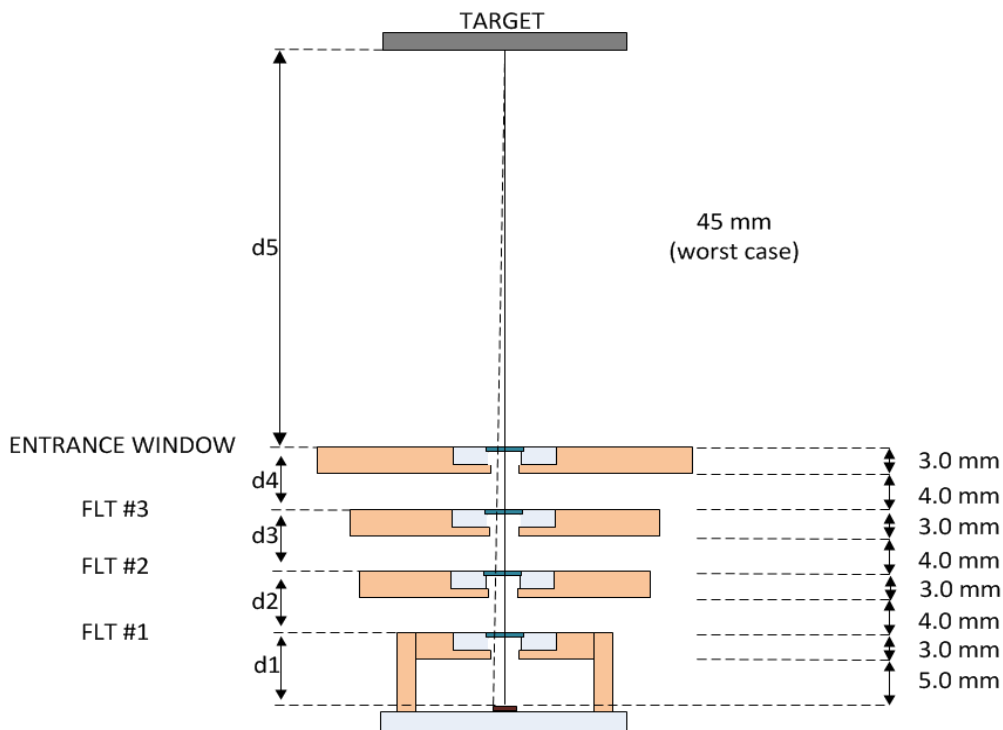
Fig. 5.3.1: baseline optical scheme (distances not to scale)

The radiation from the target passes through an entrance window (which also has the capability to sustain the ambient-vacuum differential pressure) and then through a set of optical filters, mounted on the snout caps, prior to reach the detector.

Optical Filters mounting scheme: the inner filters will be assembled (glued) onto a frame, an annulus with external diameter 11.0 mm and internal diameter 3.7 mm. Each annulus will be hosted on a proper recess (seat) on the related snout cap, the optical aperture of the stage will be imposed by the bottom aperture of the snout cap itself having circular shape and tapered edges to minimize fluorescence from the annulus walls.
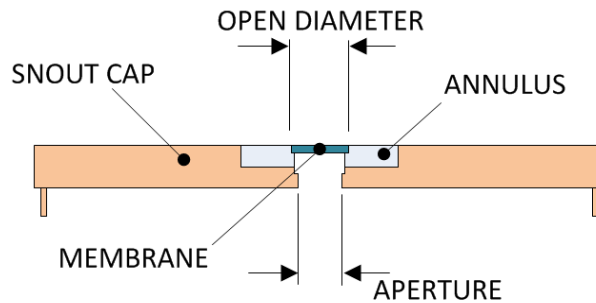
Fig. 5.3.2: Optical Filter mounting scheme and nomenclature

The entrance window will be hosted by the related front cap in a standard mount as defined by the selected primary provider (MOXTEK). Selecting the smaller "standard" window from the provider, we set the open diameter to 4.9 mm, which would lead to a counterbore diameter of 5.9 mm assuming epoxy bonding

Fig. 5.3.3: standard mount for the Be window (entrance window) from the company MOXTEK

The following table reports the relevant data.

OPEN

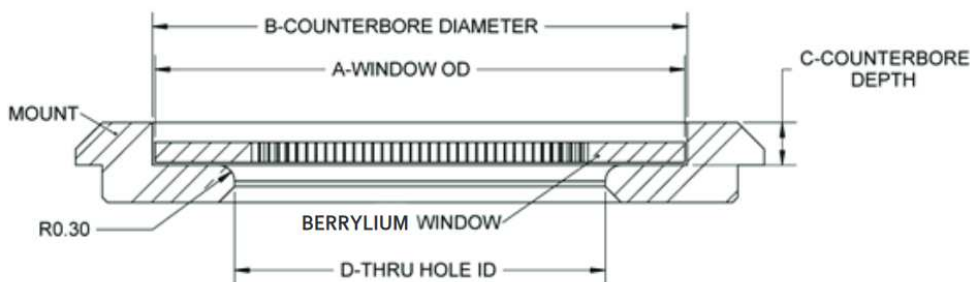| Item	Parameter	Value	Remarks
External Window (EW)	Aperture diameter	4 mm	Aperture and open diameter are selected in function of commercial availability
	Open diameter	4.9 mm	
	Coaxial error	< 0.5 mm	w.r.t detector center
	Operating temperature	~300 K	Ambient temperature
	Membrane material	Be+protective coating	Be thickness 8 μm
	Frame material	Stainless steel	
	Differential pressure	< 10^5 Pa	Ambient-vacuum He leak < 1e-7 Pa·L/s
	d5	45 mm	TARGET-EW distance (distance from detector: 29 mm)
Inner Filter (FLT#1)	Aperture diameter	3 mm	
	Open diameter	3.7 mm	
	Coaxial error	< 0.5 mm	w.r.t detector center
	Operating temperature	75 mK +/- 25 mK	
	Membrane material	Al-coated polyimide	500 nm PI, 50 nm Al
	Frame material	Copper	
	Differential pressure	< 10^3 Pa	Requires venting provision in the snout/bridge
	d1	8 mm	DETECTOR-FLT#1 distance
Inner Filter (FLT#2)	Aperture diameter	3 mm	
	Open diameter	3.7 mm	
	Coaxial error	< 0.5 mm	w.r.t detector center
	Operating temperature	4 K +/- 2 K	
	Membrane material	Al-coated polyimide	500 nm PI, 50 nm Al
	Frame material	Copper	
	Differential pressure	< 10^3 Pa	Requires venting provision in the snout
	d2	7 mm	FLT#2-FLT#1 distance (distance from detector: 15 mm)
Inner Filter (FLT#3)	Aperture diameter	3 mm	
	Open diameter	3.7 mm	
	Coaxial error	< 0.5 mm	w.r.t detector center
	Operating temperature	≤ 77 K	nominal 70 K
	Membrane material	Al-coated polyimide	500 nm PI, 50 nm Al
	Frame material	Copper	
	Differential pressure	< 10^3 Pa	Requires venting provision in the snout
	d3	7 mm	FLT#3-FLT#2 distance (distance from detector: 22 mm)
	d4	7 mm	EW-FLT#3 distance

OPEN

Additional requirements:

- Internal filter annuli dimensioning: external diameter 11 mm (+ 0, -0.05), internal diameter 3.7 mm (+0, -0.05), thickness between 0.8 mm and 1.5 mm.
- Internal filter seating (on the snout caps): diameter 11.2 mm (+0.05, -0).
- Shroud-filter interfaces shall provide a good thermal conductance.
- Maximum photon shot noise on the full filters stack: 0.5 eV FWHM (equivalent energy degradation).
- Minimum X-ray transmission on the full filter stack: 0.15 @ 1 keV, 0.7 @ 2 keV, 0.95 @ 4 keV.
- Surfaces finishing: bottom cap surfaces, snout internal walls – low emissivity (polished); upper cap surfaces – low reflectivity (not polished, roughened/blackened).

The following optimizations are not in the baseline, but can be implemented if the need arise to further decrease the photon shot noise onto the detector:

- Baffles may be added on the caps, limiting the higher temperature surfaces visible by their filter to the respective hotter filters.
- Baffles and upper cap surfaces could be coated with IR absorbing material.
- Filters could be mounted with a small tilt (2°) w.r.t. the detector plane, in alternate directions, to reduce the contribution of IR multiple reflections.

5.4   Magnetic shielding and fine control requirements

Superconductors devices are intrinsically sensitive to magnetic fields so that it is important to provide an adequate shielding around the active devices in the cold head.

The guideline requirement for residual static or low frequency magnetic field within the cold head is:

$$B < 1 \ \mu T$$

This means a shielding factor at least 50 w.r.t. the earth magnetic field and any comparable stray field at the instrument site.

To provide the main B attenuation It is required to implement a superconducting enclosure (typically Nb, but Al also is effective at temperatures 1K or lower) covering the detector area and possibly (TBC) the whole cryogenic chipset.

The baseline design foresees the use a superconductive layer (e.g. Sn/Pb alloy) on the 4K shroud with the precaution to leave a "slit" along the part of the length of the cylinder to avoid flux trapping.

OPEN
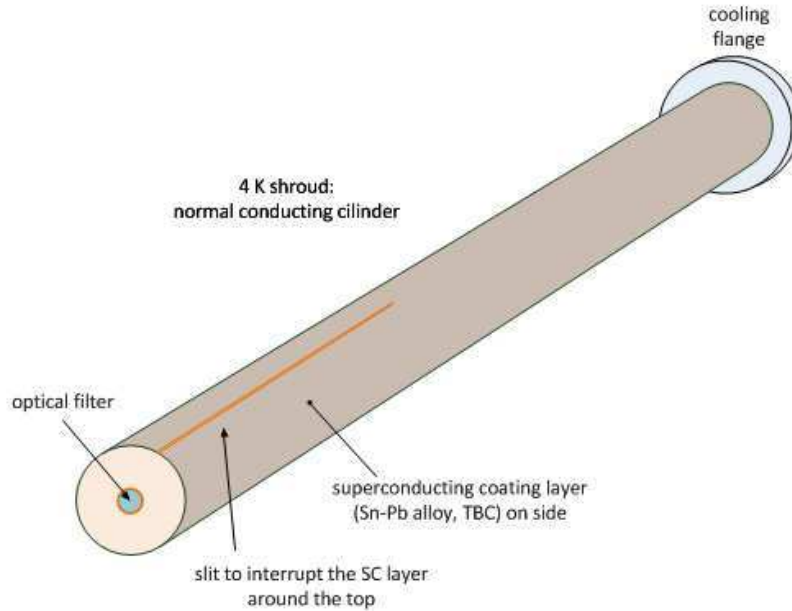
Fig. 5.4.1: SC magnetic shield @ 4K (concept)

The front cap (hosting the filter) will not be superconductive to avoid distortion of the field from the coil.

An additional room-temperature shield will be provided as a mu-metal "sock" to be pulled on the snout during cooldown and then removed when reached the operating temperature.

5.4.1 Magnetic coil

It should also be noted that the performance of the detector depends on the bias point and that changes with B-field. The introduction of an Helmholtz coil is envisaged to allow fine adjustment of the residual B field for maximum performances.

Such coils should be capable to generate a field in the order of few µT very uniform across the detector surface.

The following figure shows a coil as used in SRON and available for the project:

Fig. 5.4.1.1 example of coil used in SRON

The coil is connected by means of two wires to the small PCB hosting the connector on the detector holder. From there the signal will be routed through a superconducting loom. The traces and/or solder pads should be tinned, such that this provides a very low resistance and hence dissipation once the tin becomes superconducting.

The following table parameter gives some relevant coil data.

Parameter	Value	Remark
Coil thickness	1.15 mm	
Coil outer diameter	20.4 mm	
$N_{windings}$	600	NbTi wiring copper cladding
wire size	50 µm	(66 µm including insulation)
Distance to TES center	< 6 mm	
Expected field	~ 20 µT/mA	at detector chip center
Required Bz field	TBD	depending on operating condition
Expected max current	< 10 mA	Limit dissipation (contact resistance)

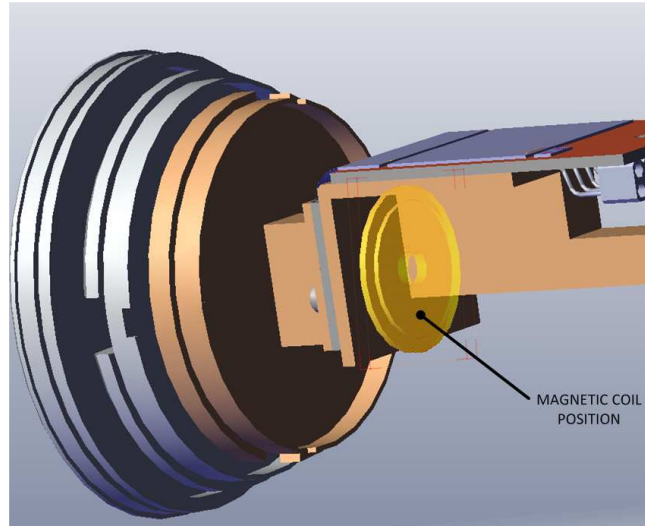Table 5.4.1.1 Coil design parameters

OPEN

Fig. 5.4.1.2 Envisaged position for the coil
just below the detector chip on the detector holder

5.4.2 Precautions to maintain magnetic uniformity

Magnetic uniformity is very important as the baseline design only foresees one coil for the full array. The mu-metal sock outside of the snout will attenuate external magnetic fields within the experiment during cooldown. The superconducting Sn/Pb layer on the 4K shroud freeze the residual magnetic field when it transitions trough the critical temperature. This implies that any part with a residual magnetic moment, could probably create a non-uniformity in the magnetic field over the TES array.

To characterize these effects some parts normally used in these set up have been measured for residual magnetism at room temperature by means of a Bartington fluxgate sensor. This holds for the NbTi looms with CuNi cladding, a part PCB with gold plating (over a nickel barrier), connectors as well as resistors. The components were magnetized with a magnet, and the residual field was measured. Only the connectors had a little higher residual magnetic field, but they were already not used close to the detector for this very reason. Non magnetic resistors (without a Nickel barrier) are not available in the low resistance value such as the shunt resistor. However, a distance of 10mm seems sufficient to make it below the detection threshold.

This does not necessary imply that these components do not change the magnetic field, but this is much harder to measure. For example it is not very clear how the superconducting looms within the magnetic field of the coil could alter this field. Therefore it might be important to route these looms outside the coil center as much as possible and make sure they will not be able to move. Tin should be avoided as much as possible close to the detector array, as it is a superconductor @ 50mK and can therefore significantly alter the magnetic field.

5.5 Electrical connections and CRYO-HARNESS

Purpose of the cryo-harness is to provide the electrical connections between the low-temperature sections within the cryostat and the connectors at the cryostat top flange.

These electrical functions are to be fulfilled while at the same time minimizing the heat conduction from the warm environment to the cold sections and the heat dissipation from the resistive impedance of the cable itself.

Moreover to limit propagation of EMC disturbances inside the shielded vessel it is mandatory to provide adequate shielding of those cryo-harness sections which carry AC signals e.g. the TES AC biasing used for FDM muxing and the related multiplexed signal outputs.

The design of the harness has to be tackled at an early stage as it will condition the overall harness arrangement and routing.

The choice of each wire material composition and geometry (gauge/length) has to carefully take into account the maximum electrical current expected, both while at cold or during warm dry-testing of the system.

In the design of the cryo-harness it is also important to establish an optimum redundancy philosophy to be resilient to possible wire breakage.

At the probe front side the cryo-harness will require a short-length interconnections between the devices to be implemented using superconductive wires, in particular the circuitry related to the FE SQUID and the AMP SQUID foresees the following scheme:
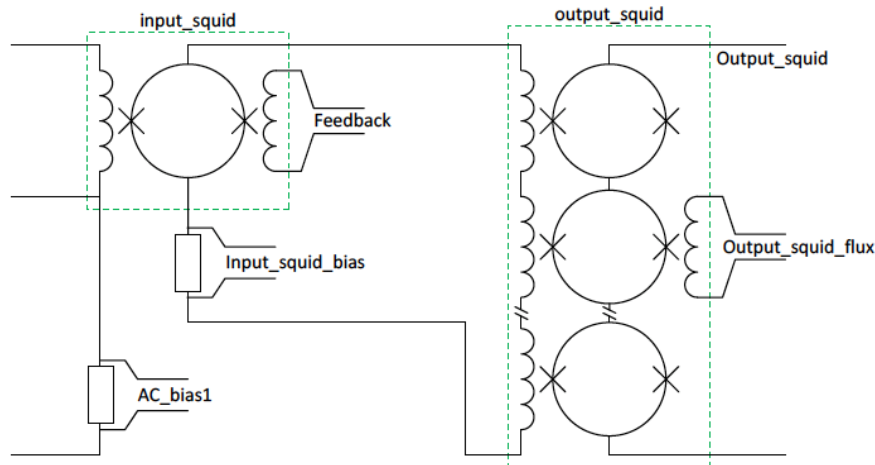

Fig. 5.5.1: Circuit diagram of the SQUIDs bias and interconnections.

The following picture shows a preliminary description of the cryo-harness and also internal connections between the various cryogenic elements: it is given here to show the level of complexity, number of wires, various temperature stages etc. and is not meant to be the actual electrical design.
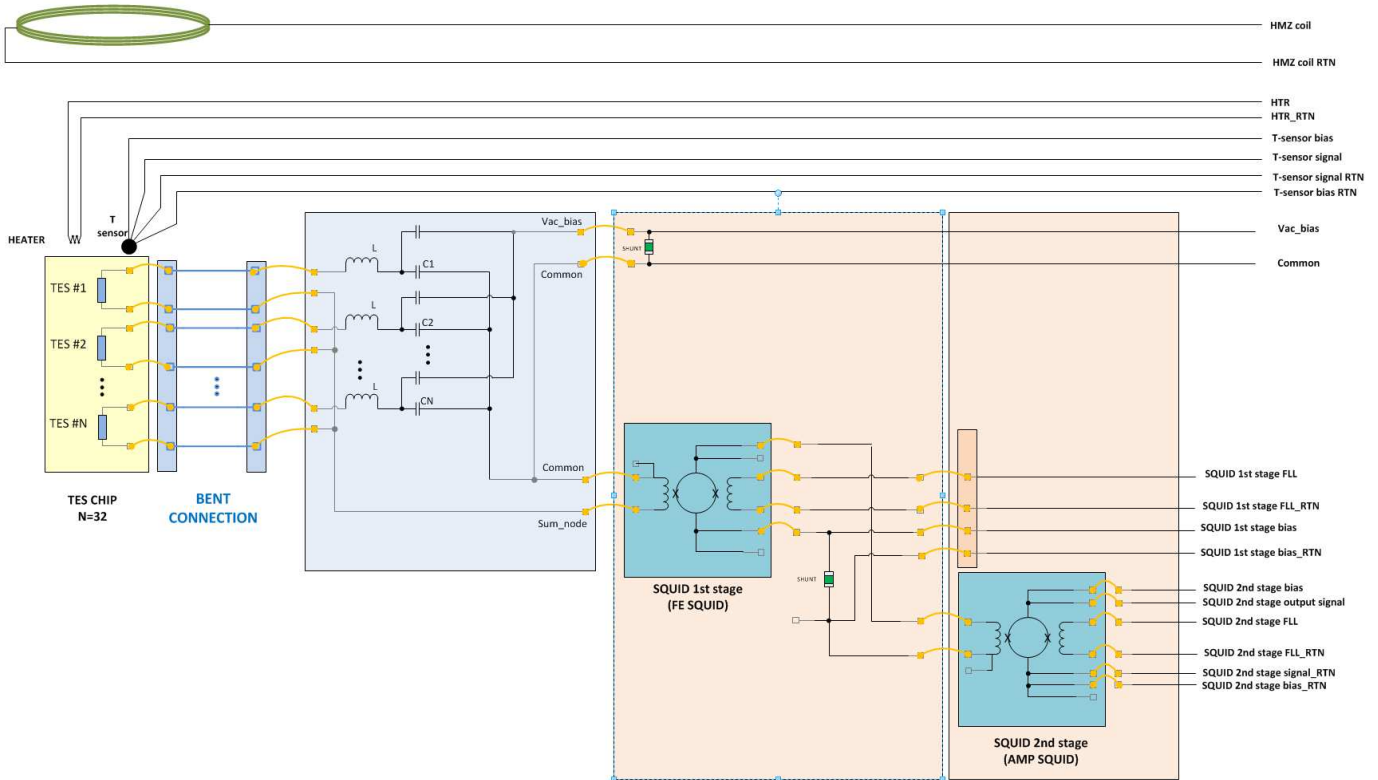
OPEN

Fig. 5.5.2: sketch of the internal connections (concept)

Notes:

1. The chips shall be thermally connected to the cold finger, in the SRON setup this is done using clamps for all chips but for the SQUID chips which are glued.

2. The metallic structure shall include "cavities", depth TBD mm, below the active part of the chips to minimize stray capacitive coupling.

3. The "bent connection" is geometrically convenient when placed between the TES chip and the LC chip. The envisaged connection is by SRON design composed by a rigi-flex structure with silicon-made rigid section and a polymide flex section with superconductive tracks. A dedicated design will address minimization of lateral dimensions.

4. The chips are interconnected between each other (detector, LC, 1st SQUID) via wire bonding

5. A small rigid PCB on the detector holder provides pads to connect the relevant chips via wire bonding and a miniature connector to mate with the cryo-harness

OPEN

6. The 2nd stage SQUID (AMP SQUID) is hosted on a small PCB on the "1K" stage and connected to the 1st stage SQUID by a couple of superconductive wires through miniature connector.

7. Connectors are foreseen to allow easy removal of the Detector Holder assembly for maintenance or modification/substitution

8. The prototype spectrometer will follow the SRON set-up where there is no local connection to GND in the cold, all "RTN" wires are floating in the cryostat and the grounding is done in the warm electronics.

In the following a very preliminary description of the cryoharness is given with the purpose to visualize its elements and features.

In particular the conductors materials, cross-sections and length of the various elements are specified in section 5.5.1 for each line taking in account the needed current capability and thermal load constraints.

Superconductor wires are needed at the lower T to reduce heat load on the cold tip, while fair electrical conductors with poor thermal conductivity like stainless steel or manganine could be used for the other segments.
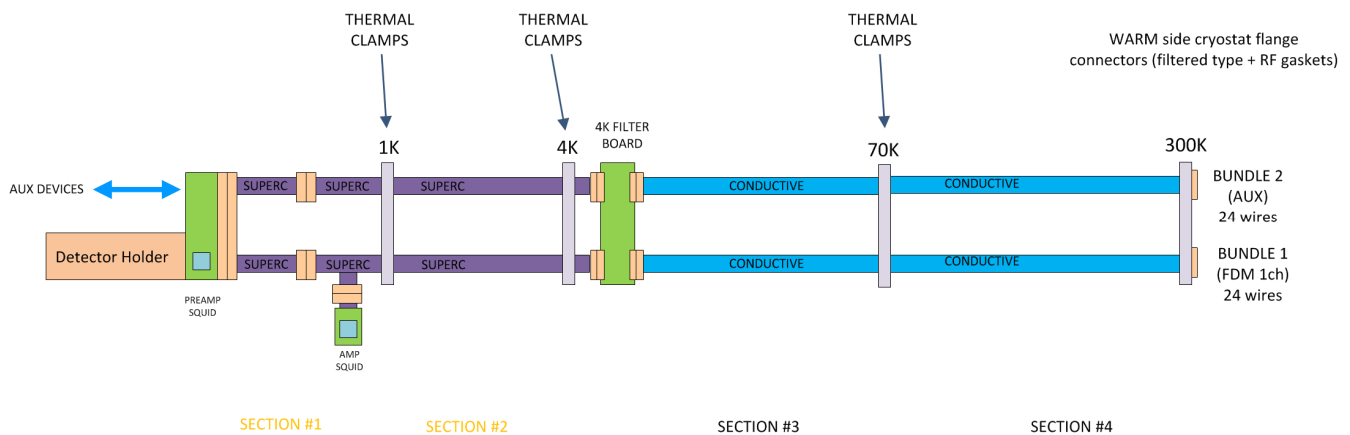

Fig. 5.5.3: sketch of a possible cryoharness (TBC)

Main features:

The cryoharness connects the 300K flange with the Detector Holder i.e. down to the 50 mK base temperature.

It will be subdivided into 2 bundles, one dedicated to the FDM readout and the other for ancillary services (e.g. thermometry, coil).

Each bundle is thermally subdivided in 4 sections, each one thermally clamped at both ends to a suitable thermal well.

The two lower temperature sections should be superconductive, thermally clamped at 4K and 1 K on the higher T sides and on the cold tip on the lower T side.

A filter board shall be foreseen at the 4 K level.

A sketch (only to illustrate the concept) of the lower-T section is:
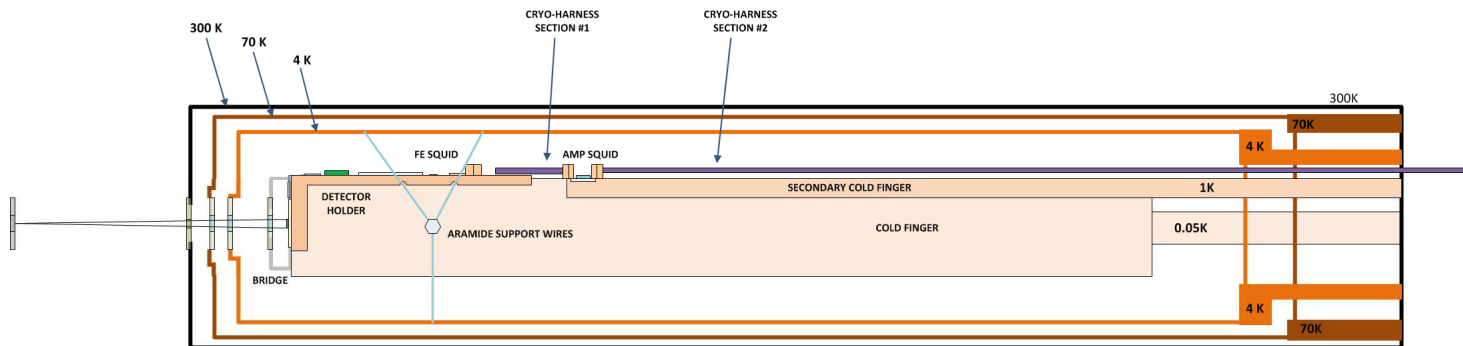

Fig. 5.5.4: sketch of the snout showing cryoharness sections #1 and #2

The following table gives an indication on the typical current capabilities required by various cryoharness lines.

Parameter	Direction	Range	Unit	EGSE parameter	Remark
OUTPUT_SQUID	FEE-in		[Ohm]		Depending on set input impedance
	FEE-out	± 350	[µA]	ArraySquid Bias	
		+ 39	[mA]	Deflux_2	at 50 Ohm
OUTPUT_SQUID_FLUX	FEE-out	± 100	[µA]	flux2	
INPUT_SQUID_BIAS	FEE-out	± 350	[µA]	PreSquidBias	
		+ 39	[mA]	Deflux_1	at 50 Ohm
FEEDBACK	FEE-out	± 100	[µA]	flux1	
TES_AC_BIAS1	FEE-out				Generated by DEMUX
MAGNET	FEE-out	± 2.4	[mA]	LP_magnet	
		± 50	[mA]	HP_magnet	
50mK_THERM_V	FEE-in	~ 2	[mV]		
50mK_THERM_I	FEE-out	± 11	[nA]		
TES_AC_BIAS2	FEE-out				Generated by DEMUX
HEATER	FEE-out	± 100	[µA]		

Table 5.5.1: typical cryo side current ranges

The requirements for each section/wire in the are collected in tables in the following paragraph.

OPEN

5.5.1 Wiring tables (signal ID, current range, DC resistance (at warm and at cold)

SECTION #1			
Tlow	[K]	0.05	
Thigh	[K]	1	
Length	[m]	0.1	
wire material		NbTi	
diameter	[m]	1.00E-04	AWG38
section	[m²]	7.85E-09	
Cold ohm/m	[ohm/m]	0	
Troom ohm/m	[ohm/m]	50	
Cold th cond	[W/(m·K)]	0.027	
Cold Resistance	[ohm]	0	
Troom Resistance	[ohm]	5	
# of wires			max curr
			[A]
2	COIL		2.40E-03
2	TES AC BIAS		1.00E-03
2	HEATER		1.00E-04
2	Tsensor bias		1.10E-08
2	Tsensor signal		1.00E-09
2	PE SQUID FLL		3.50E-04
2	PE SQUID BIAS		3.50E-04
2	AMP SQUID FLL	n/a	
2	AMP SQUID BIAS	n/a	
24	GND/GUARDS		0.00E+00

Table 5.5.2: data for section #1

OPEN

SECTION #2

Tlow	[K]	1	
Thigh	[K]	4	
Length	[m]	0.3	
wire material		NbTi	
diameter	[m]	1.00E-04	AWG38
section	[m²]	7.85E-09	
Cold ohm/m	[ohm/m]	0	
Troom ohm/m	[ohm/m]	50	
Cold th cond	[W/(m·K)]	0.027	
Cold Resistance	[ohm]	0	
Troom Resistance	[ohm]	15	

# of wires			max curr
			[A]
2	COIL		2.40E-03
2	TES AC BIAS		1.00E-03
2	HEATER		1.00E-04
2	Tsensor bias		1.10E-08
2	Tsensor signal		1.00E-09
2	PE SQUID FLL		3.50E-04
2	PE SQUID BIAS		3.50E-04
2	AMP SQUID FLL		3.50E-04
2	AMP SQUID BIAS		3.50E-04
24	GND/GUARDS		0.00E+00

Table 5.5.3: data for section #2

OPEN

SECTION #3

		CuNi	Cu
Tlow	[K]	4	
Thigh	[K]	70	
Length	[m]	0.35	
wire material	(2 types -->)	CuNi	Cu
diameter	[m]	1.00E-04	
section	[m²]	7.85E-09	
Cold ohm/m	[ohm/m]	2	7.2
Troom ohm/m	[ohm/m]	2	7.2
Cold th cond	[W/(m·K)]	386	
Cold Resistance	[ohm]	0.7	2.52
Troom Resistance	[ohm]	0.7	2.52
# of wires			max curr
			[A]
2	COIL	Cu	2.40E-03
2	TES AC BIAS	Cu	1.00E-03
2	HEATER	Cu	1.00E-04
2	Tsensor bias	Cu	1.10E-08
2	Tsensor signal	CuNi	1.00E-09
2	PE SQUID FLL	Cu	3.50E-04
2	PE SQUID BIAS	CuNi	3.50E-04
2	AMP SQUID FLL	CuNi	3.50E-04
2	AMP SQUID BIAS	Cu	3.50E-04
24	GND/GUARDS	CuNi	0.00E+00

Table 5.5.4: data for section #3

OPEN

SECTION #4

		CuNi	Cu
Tlow	[K]	70	
Thigh	[K]	300	
Length	[m]	0.35	
wire material	(2 types -->)	CuNi	Cu
diameter	[m]	1.00E-04	
section	[m²]	7.85E-09	
Cold ohm/m	[ohm/m]	2	7.2
Troom ohm/m	[ohm/m]	2	7.2
Cold th cond	[W/(m·K)]	386	
Cold Resistance	[ohm]	0.7	2.52
Troom Resistance	[ohm]	0.7	2.52
# of wires			max curr
			[A]
2	COIL	Cu	2.40E-03
2	TES AC BIAS	Cu	1.00E-03
2	HEATER	Cu	1.00E-04
2	Tsensor bias	Cu	1.10E-08
2	Tsensor signal	CuNi	1.00E-09
2	PE SQUID FLL	Cu	3.50E-04
2	PE SQUID BIAS	CuNi	3.50E-04
2	AMP SQUID FLL	CuNi	3.50E-04
2	AMP SQUID BIAS	Cu	3.50E-04
24	GND/GUARDS	CuNi	0.00E+00

Table 5.5.5: data for section #4

OPEN

5.5.2 Looms

The detector-related cryoharness will be built using looms, the looms will carry the thermometry signals but also the detector signals and biasing from 300K to the detector.

The spectrometer has two types of looms:

- Hybrid Cu/CuNi loom. It is a loom of which a few wires made of coper and the rest of the wires are made of copper/nickel. This loom is placed between 300K and 4K stage (section #3 and #4). Also uniform PhBr looms (phosphor bronze) could be used for this stage.

- NbTi loom. It is a loom of which the wires are made of niobium titanium. This loom is placed between 4K and mK stages (sections #1 and #2) because it is superconducting when the cryostat is cooled down.
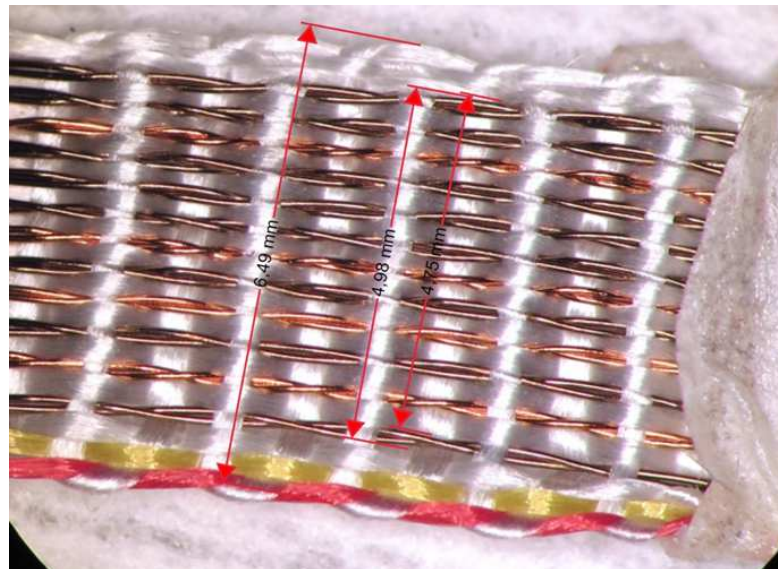

Fig. 5.5.2.1: Example of a loom with relevant dimensions (manufacturer Tekdata Cryoconnect)

Each loom contains 12 pairs of wires. That is in total 24 wires in each loom. The thickness of each wire is 100 um (AWG38). The looms are connected on both ends to a connector soldered on a PCB. These will be called loom PCB's.

Fig. 5.5.2.2: example of a loom including its loom PCB

5.5.3 Connections scheme

All the looms contain a loom PCB with a header on one end and a socket on the other end. It does not matter which type of loom is used because the wiring on the PCB's is the same.
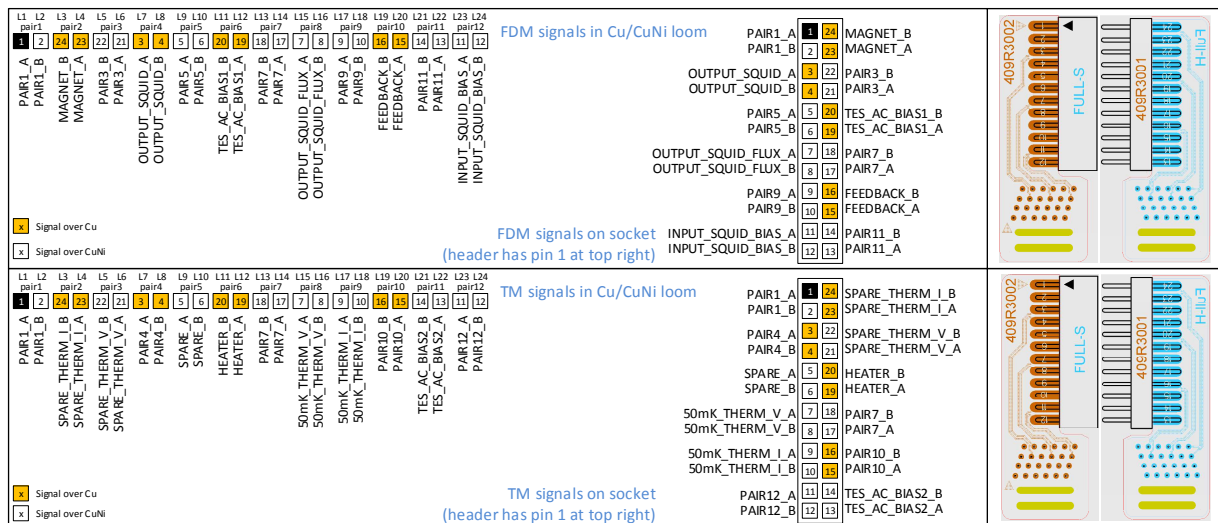

Fig. 5.5.3.1: pin-out of the loom PCB

FDM loom signals are meant for the detectors, while TM looms are meant for the thermometry.

5.5.3.1 Connection overview

The looms will be read out by the FEE.

The connection overview can be found in Fig. 5.5.3.1.1.

At 300K, the FDM and TM loom signals will go through a FEE Interface PCB (609R3007). This PCB translates the detector pinout to the FEE pin out. This part is described is chapter 5.7.1.

After this translation, the looms will be thermalized and filtered at the 4K stage with the TES_4K_SignalFilter II board (409R3004). This PCB is described in chapter 5.5.5.

The FDM loom contains signals that have to be routed to the 1st stage and 2nd stage SQUID. Because the 1st stage squid and 2nd stage squids will be located at different temperature stages, the looms signals have to be split. This function is insured by the loom attached to J10.6A,B and D. The loom that is used to connect the second stage SQUID has also to carry the thermometry. Therefore, The TM loom signals have to be combined with the 2nd stage SQUID signals. This function is insured by the loom attached to J10.7, J10.8 and J11.8.

The wiring scheme of the looms can be seen in Fig. 5.5.3.1.2.

Fig. 5.5.3.1.1: Loom connection overview.

OPEN

Template 83230326-DOC-TAS-EN/003

Fig. 5.5.3.1.2: Loom wiring scheme

As described in the following Fig. 5.5.3.1.3, the connection from the looms to the SQUIDs will be realized with a 2 PCBs. One PCB for the connection to the 1st stage SQUID and a second PCB for the 2nd stage SQUID. Fig. 5.5.3.1.4 shows the schematics of those 2 PCBs.

Fig. 5.5.3.1.3: SNOUT front end wiring scheme

OPEN

Fig. 5.5.3.1.4: SQUID bonding PCBs

5.5.4 Looms routing and thermal clamps

The looms between 300K and 4K will be routed within the cryostat along a path chosen to ensures minimization of interference and the correct thermal anchoring at the selected thermal wells.
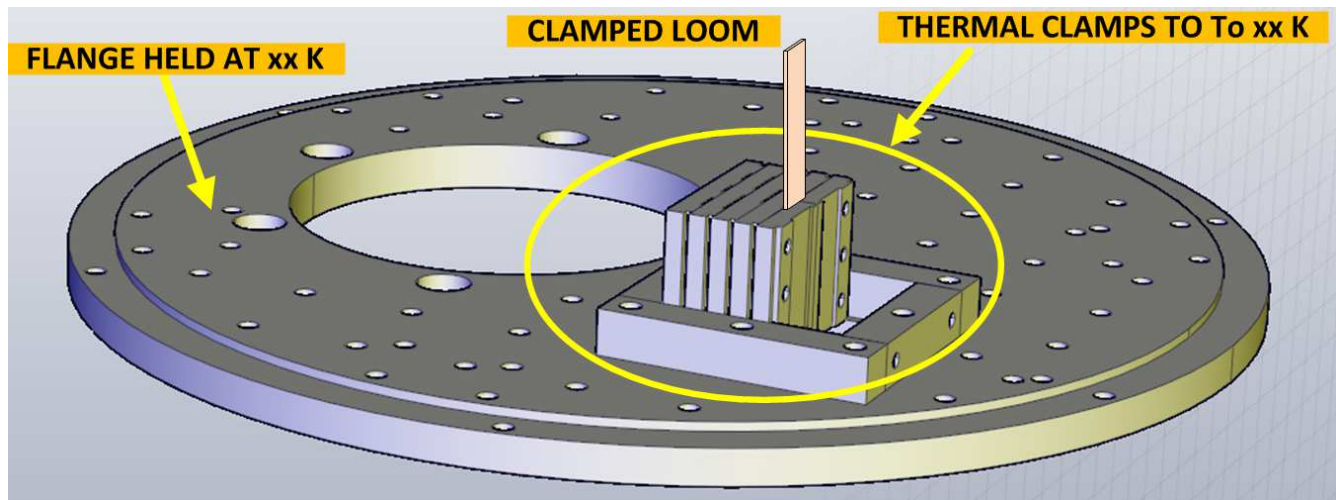

Fig. 5.5.4.1: example of the envisaged thermal clamp

5.5.5 EMC filters

Radio Frequency (RF) interference is a well-known issue when working with so high sensitivity devices like the SQUIDs. On the other hand their use requires complex and often large cryostats with long section of harness running from the cold section to the warm section, a feat that increase the risk for RF interferences.

This task goes together with an overall interference control plan at system design level, including the use of continuous (i.e. not braided) shielding and minimization of connection length from the cryogenic environment and the warm front-end level.

To tackle these problems it is required the design of RF filters in the MHz frequency range located within the cryostat and capable to operate at cryogenic temperature down to 1 K while providing a large enough attenuation of any interfering signal that could couple with the harness.

All looms are thermalized at the intermediate board. The interconnection PCB board at 4K also has simple RC filters (example schematics in Fig. 5.5.5.1, R=1Ω, C=6.8PF). This is to protect the experiment from high frequency noise that can couple to the wires at warm electronics.
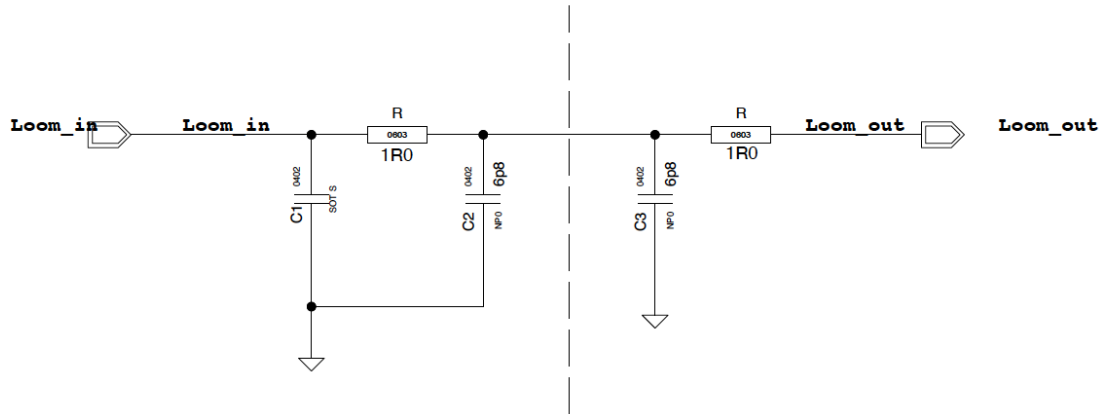
OPEN

Fig. 5.5.5.1: schematic circuit of the filter boards at 4K stage.

5.6   Cryogenics cooling system requirements

The cryogenic cooling system shall provide the cooling power to the various section within the cryostat. There are many possible cooling schemes and the final choice should be dedicated to the particular application. However, in general, any cryoharness will be thermally anchored at every temperature stage in the cryostat. The available cooling powers for thermal anchoring are approximately as follows:

- 1st stage pulse-tube 70 K, ~ 5 W
- 2nd stage pulse-tube 4 K,   ~ 50 mW
- 1 K stage flange 1 K,   ~ 50 µW
- 100 mK flange 100 mK,   < 1 µW

The above cooling stages and powers must be used for the following sections of the harness:

- Detector cold head (TES reference bath)
- Cold Front End Electronics (SQUIDs, filters)
- Lower temperature section of the cryoharness
- Intermediate flanges for heat sinking (cold head shields and cryoharness attachment points)

OPEN

5.7   Warm Electronics requirements

The Warm Electronics directly interfaces the analog signals from the Cold Front End Electronics and provides the interface for bias and signals to/from the cold head.
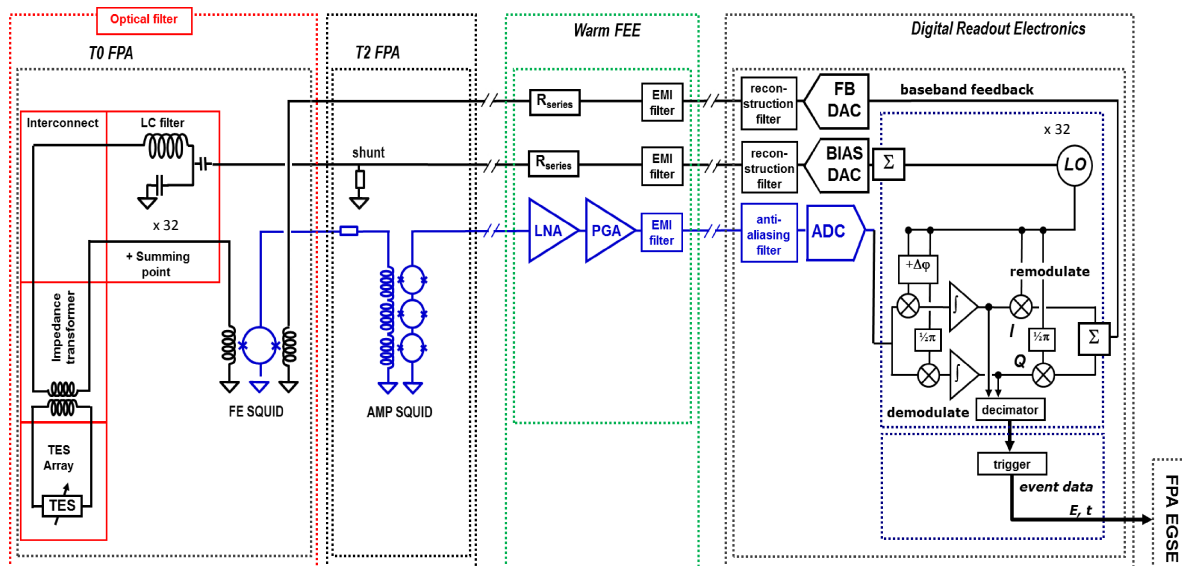

Fig. 5.7.1: Block Diagram of the warm readout electronics

The warm electronics, will be SRON-developed lab electronics functionality is split over two units (see Fig.5.7.1):

1) An analog electronics unit (the FEE, or Front End Electronics) located on the cryostat and containing:
   - a low-noise amplifier (LNA) for the output signal, plus an additional Programmable Gain Amplifier (PGA)
   - analog bias supplies for the SQUID amplifiers,
   - Buffers and range switches for AC bias signals
   - Heater drive
   - Cryogenic temperature sensor readout
   - PID temperature controllers
   - B-field coil drive
   - feedthrough filters of all electrical lines entering the detector's Faraday cage.

2) A digital electronics unit (Demux) contains the digital signal processing that is required to
   - generate the AC carriers,
   - digitize and demodulate the output signal,
   - generate the baseband feedback signal that is required to null the AC carriers at the input to the FE SQUID, and process the demodulated output signal to generate events that can be processed offline.

OPEN

The system also comes with a set of auxiliary items as:

Demux rack: The demux rack is a 19" rack containing two demux modules, and a number of DC/DC power supply modules.

PC: The PC used for the warm electronics runs the Linux operating system and SRON software for the control of the instrument, and for storage, processing and display of instrument data. It is a requirement that this PC has a connection to the internet to allow remote access from SRON, and for the network time protocol (NTP).

Cables: The cables between FEE and demux rack are specific copper wire cables with a length of 3m. The cables between demux rack and PC are optical fiber cables with a length of 10m, but cables with a length up to 100m can be used.

5.7.1 FEE box – Cryostat interface

The envisaged solution is to provide a "Mating Cylinder" between the FEE box and the cryostat designed so to make the FEE electrically part of the cryostat Faraday cage.
Massimo confirms that as far as the "flag" mounting of the FEE is on the opposite side of the cryostat w.r.t. the snout it will be OK for the LABEC set up.
Many mechanical detail are under definition, in particular the mating cylinder will be vacuum tight and provided by gaskets to make the whole assembly EMI clean.
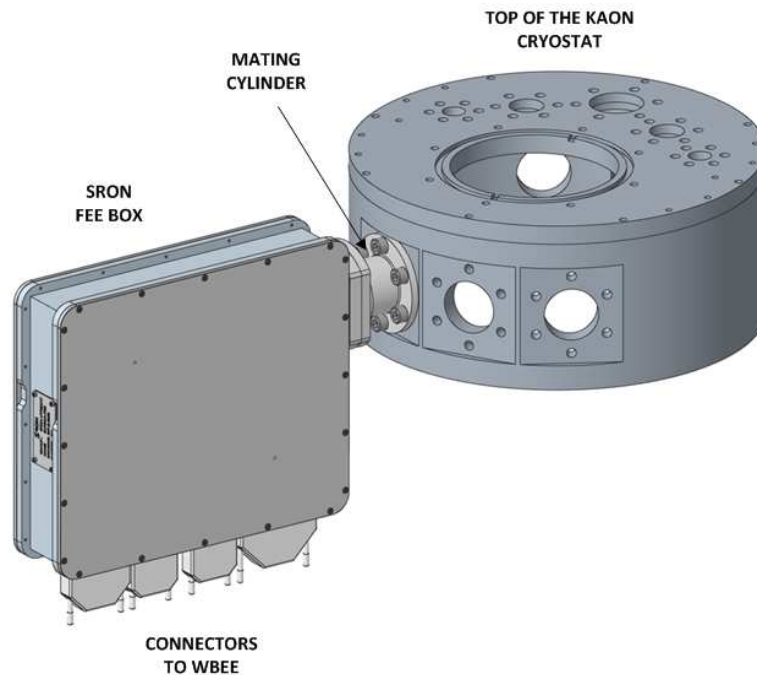

Fig. 5.7.1.1: FEE-Cryostat mating

OPEN

The interconnection part is vacuum tight and provides EMI shielding. The two looms that carry the signals between the FEE and the cold electronics are feed through potted cylindrical inserts.
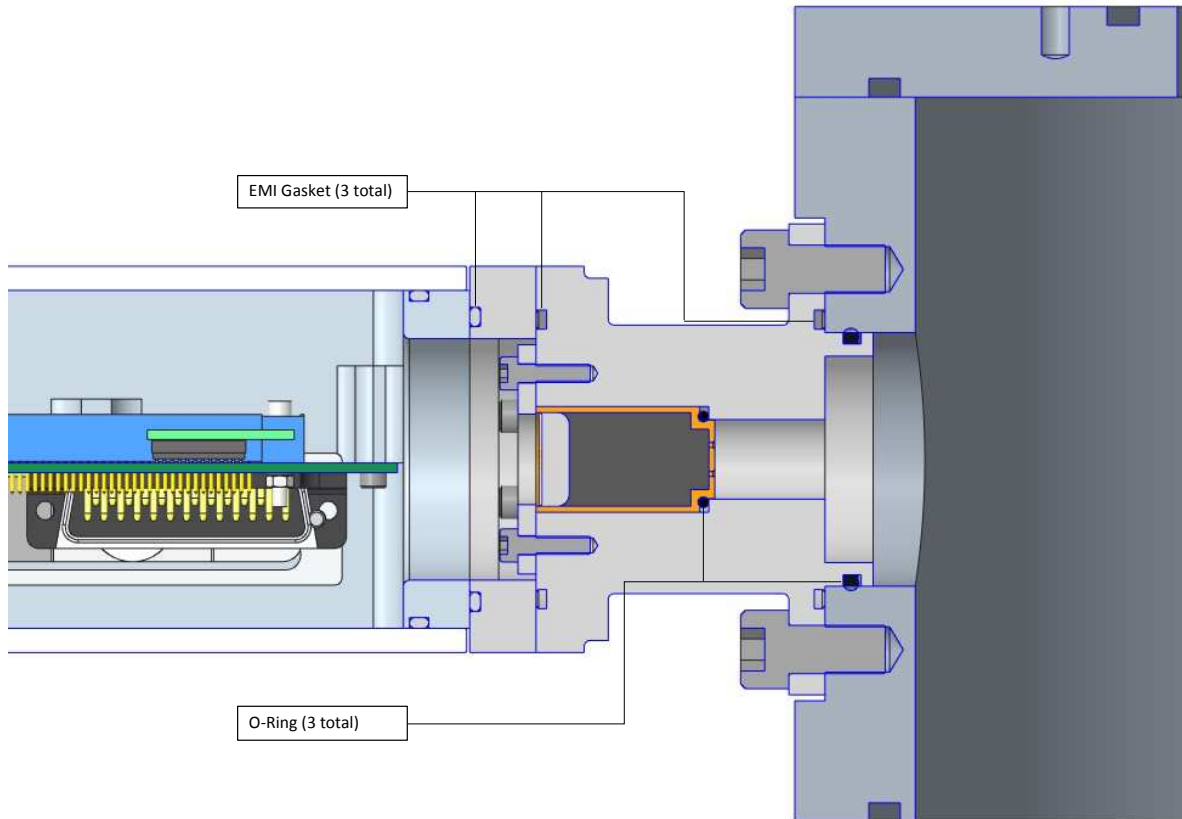

EMI Gasket (3 total)

O-Ring (3 total)

Fig. 5.7.1.2: section view of the FEE-Cryostat mating

5.7.1.1   Electrical interface

The FEE will readout the squids. The scheme can be found in figure 5.7.1.1.1.

Fig. 5.7.1.1.1: Scheme of the FEE

The FEE interface PCB will translate the Looms signals to the FEE signals. The scheme of this PCB is shown in the fig 5.7.1.1.2.
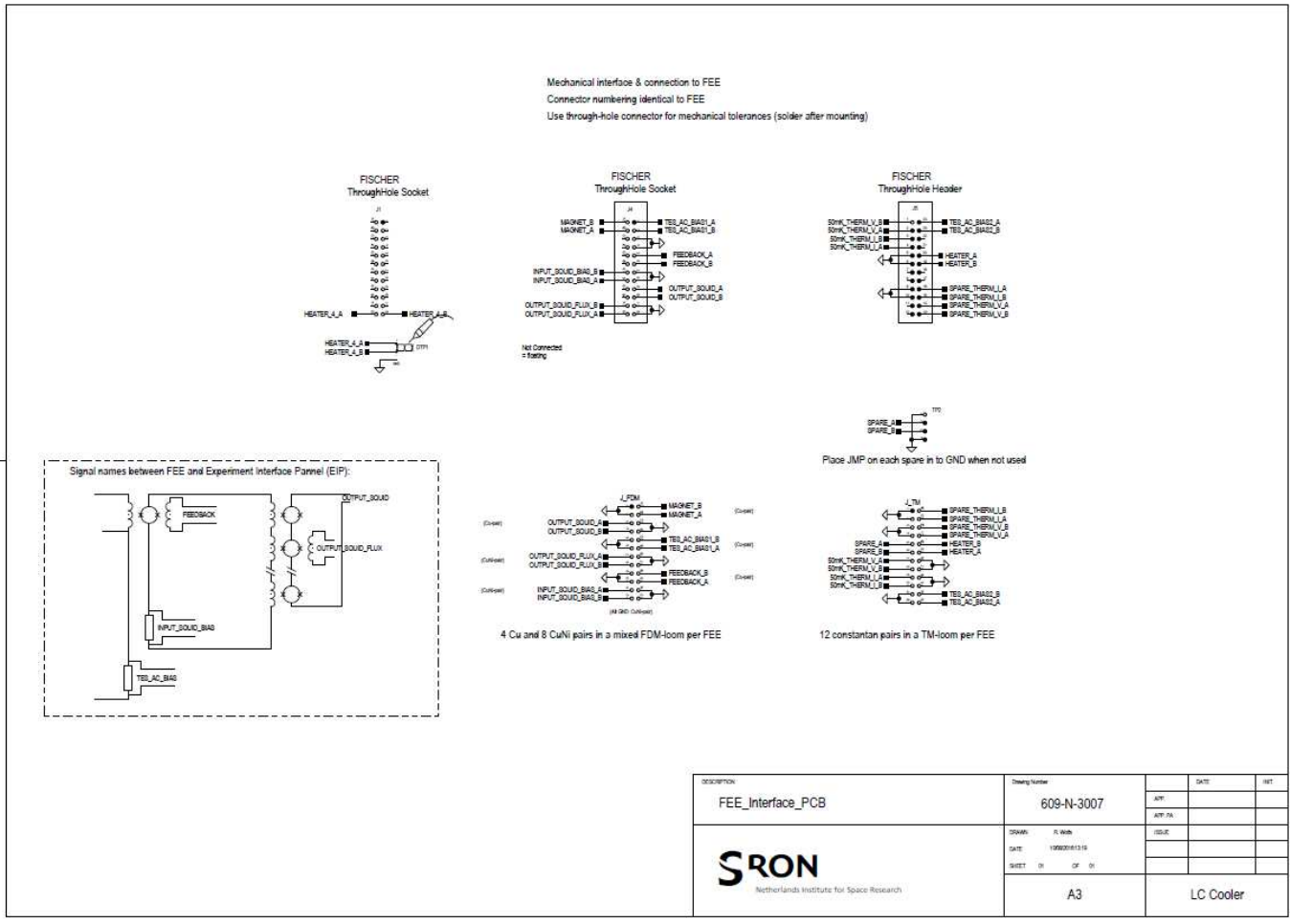
OPEN

Fig. 5.7.1.1.2: Scheme of the FEE interface PCB

5.8   End-to-End readout electronics requirements

As shown in the previous chapters the detector system studied in WP15.2 requires a complex readout which is distributed in many functional blocks along the electronics chain.

This chapter gives the guidelines to identify some important requirements which are referred to the readout chain as a whole, these shall be apportioned to each functional block in terms of "budget" in any actual system implementation.

OPEN
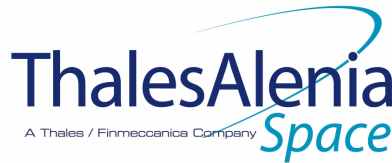
5.8.1 Dynamic Range

One important parameter that characterizes the system performance is the Dynamic Range (DR) defined as the ratio between the maximum signal range and the noise spectral density.

$$DR = As/Bn \qquad [\sqrt{Hz}]$$

Where:

As = signal amplitude (peak-to peak)
Bn = noise spectral density

The amplitude As is in expressed in units [X] (temperature, voltage, current, ….) depending on the actual system we are dealing with) and the noise spectral density Bn is expressed in units [X/sqrt(Hz)] so that the dynamic range DR is expressed in units [sqrt[Hz]. This DR parameter is somehow analogous to a relative Signal-Noise Ratio (SNR) in the sense that:

- the larger it is, the better for signal detection
- being normalized to a unity frequency bandwidth requires the specification of the actual measurement bandwidth to get absolute results

The basic DR requirement for the overall readout chain is that it shall not spoil the intrinsic DR of the detector. As a general rule, if we assume that the noise in the amplifier chain and the noise in the detector adds as squared sum, the DR of the SQUID+WFEE amplifier chain shall be at least 2-3 times larger than that of the detector.
To give some quantitative examples we note that TES detectors optimized for IR detection working around 100 mK are reported to have intrinsic DR in the range of 1e4 to 1e5 [sqrt(Hz)] [RD13] while the performances of best science-grade SQUID devices are in the order of 0.1 μΦo/sqrt(Hz) so assuming an almost linear peak-to peak range of 0.2 Φo gives a DR for these SQUIDs in the order of 2e6 [sqrt(Hz)].

5.8.2 Cross-Talk

This parameter is an important one in multiplexed systems where the separation between different readout channels is often made difficult by physical constraints like the closed spacing between detectors, the commonality of signal paths and sharing of common resources like cooling power, power supply etc. The cross-talk is defined as the ratio between the spurious (unwanted) signal Au at a given readout channel output as a consequence of a legitimate signal Ao within another readout channel and commonly expressed as a percentage.

$$CT = Au/Ao$$

A general guideline requirement for the overall readout chain is that the maximum signal in any readout channel shall not cause a spurious signal larger than the rms noise amplitude.

OPEN

As this may be not feasible in practical systems like the one we are dealing here a less conservative requirement can also be stated that a signal in any readout channel with amplitude just below the minimum detection threshold shall not cause a spurious signal larger than the rms noise amplitude. Following the less conservative approach either a cross-talk event is under the rms noise level or its originator causes a triggering and the cross talk can be taken in account by post-processing analysis.

To give some quantitative examples a soft x-ray detector with minimum detection threshold in the order of 100 eV and a rms noise in the order of 3 eV/2.35 ~1.3 eV would require CT < 1.3 % With this CT level the full-scale signals around 10 keV may generate spurious triggering above a detection threshold of 100 eV that can be recognized as spurious due to the time-position correlation with the originating event.

There are many possible cross-talk paths that have to be taken in account at system level, including at least the following:

- Thermal cross-talk at pixel level (may be important for high fill factor)
- Spill-over from neighbour frequency carriers (directly or via non-linearity by-products)
- Sum-node noise (SQUID input coil impedance to be minimized)
- Spill-over from shared supply or bias lines

5.8.3 Linearity

The linearity of the readout chain transfer response is important for FDM multiplexed systems as a non-linear distortion along a given channel may cause the insurgence of spurious frequencies (intermodulation by-products) that can interfere with nearby channels.

The most nonlinear elements in the readout chain are the SQUIDs which are intrinsically nonlinear and require a closed loop control with enough loop-gain to keep the intermodulation products under control.

5.8.4 Control Station requirements

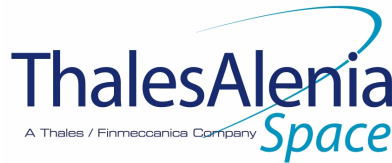The Control Station is in charge of the overall control of the instrument, namely:

- Instrument set up and commanding (cryogenics, CFEE, WFEE, WBEE)
- Instrument monitoring and control, based on the HL data
- Synchronization of all the instrument activities
- Data acquisition from detector WBEE
- Quick-Look and on-line Data Analysis features to allow inspection of the quality of ongoing acquisition
- Data format/storage to an archive for later and future analysis

The following table summarise the most important performance requirements.

OPEN

	command data rate	HK data rate	scientific data rate	storage capacity	autonomous operation	remarks
	< 1 Mb/sec	< 1 Mb/sec	< 50 Mb/sec	> 500 Gbyte	> 12 hours	

TABLE 5.10.1: orientative requirements for the control station

A modern workstation PC with suitable set of HW interfaces should fulfil the expected performances.

6. ANNEX1: PROTON BACKSCATTERING IN PIXE EXPERIMENTS

In the frame of the preliminary design of the spectrometer dealing with PIXE applications we understand that in these measurements there is a fraction of the proton beam that is backscattered from the target and could possibly propagate through the snout and affect the detector.

This is a potential disturbance to the envisaged high energy resolution measurements and has to be taken in account from the beginning either in terms of assessment of the disturbance or in terms of mitigation countermeasures to be implemented.

6.1 Assessment of the disturbance caused by backscattered protons

Assumptions:

1) We do not consider backscattered protons with < 200 keV energy

2) Protons with E > 200 keV stopped or passing through the pixel will release a saturated pulse we could disentangle from an X-ray signal

3) The saturation occurs thermally at pixel level, not in the remaining readout chain (SQUIDS and following devices)

4) Protons impinging the 300µm Si substrate (bulk or munting) will perturb the whole array as the energy release here can be as high as 3 MeV.

A preliminary analysis based on available order-of-magnitude data and simulations has been carried out considering two typical measurement scenarii:

a) Measurements on Cultural Heritage samples
b) Measurements on Aerosol samples

OPEN

The photon rate for typical settings during these measurements are:
- on the array: 1 ksps to 5 ksps
- on a single pixel: 40 to 200 sps (assume 25 pixels)

The backscattered P+/photon ratio (orientative) for typical settings during these measurements are:
- 1:100 for a Cultural Heritage campaign
- 1:10 for an Aerosol campaign

From the above data we can evaluate the proton hit rate at pixel level (assume 25 pixels) :

Proton hit rate: 0.4 cps to 2 cps per pixel (cultural heritage)
Proton hit rate: 4 cps to 20 cps per pixel (aerosol)

6.1.1 Backscattered P+ energy simulations

Some simulations for the Cultural Heritage measurements scenario are given in the table below taking in account the foreseen experimental conditions (35 mm He, 8 um Be entrance window, 2 optical filters with 50 nm Al deposited on 150 nm polymeric foil):
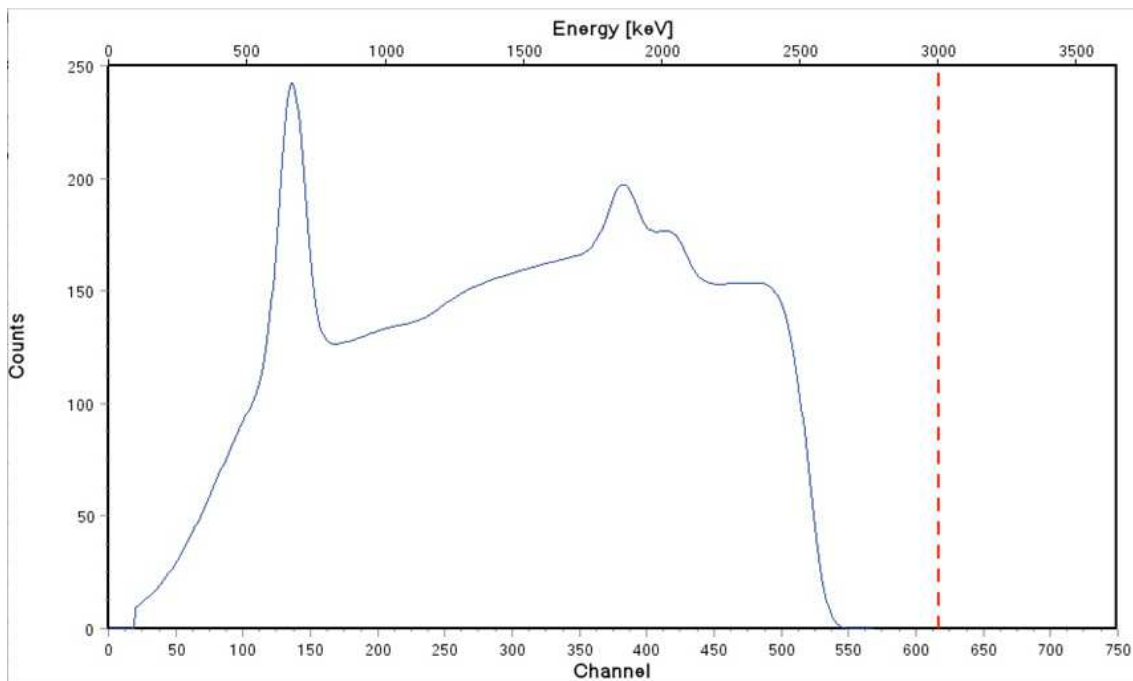

Fig. 6.1.1.1: Simulated backscattered proton energy spectrum
in the cultural heritage sample case (Roman bronze coin)

OPEN

E bin (keV)	Counts	Fraction	dE/dx (keV/um)	En.loss (keV) (in 2.3 um Au)	
0-500	3750	5.4%	206	250	(range p@525 keV = 2.3 um)
500-1000	15450	22.2%	140.1	322	
1000-1500	15200	21.8%	111	255	
1500-2000	17910	25.7%	95.1	219	
2000-2500	16850	24.2%	83.8	193	
2500-3000	420	0.6%	75.3	173	

Table 6.1.1.1: P+ backscatter ratio in a typical Cultural Heritage measurement scenario

Also some simulations for the Aerosol measurements scenario are given in the table below with the same experimental conditions as the Cultural Heritage case:
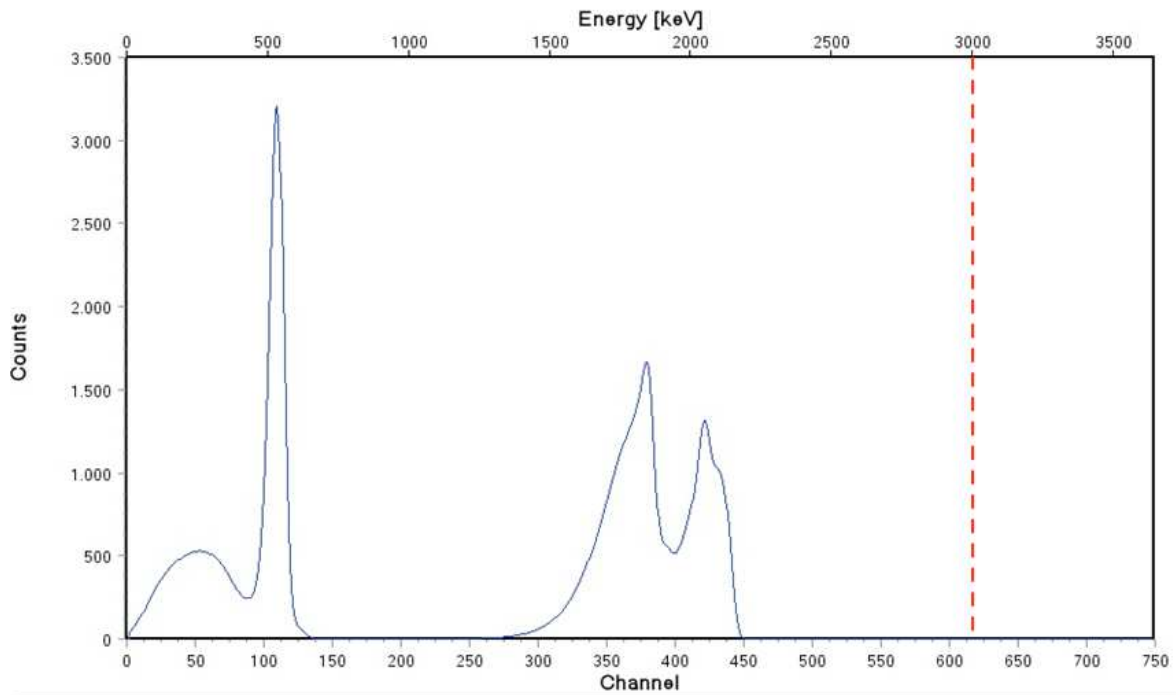

Fig. 6.1.1.2: Simulated energy spectrum of backscattered protons reaching the sensor in the atmospheric particulate matter (aerosol) sample case (PM2.5 on Teflon filter)

OPEN

E bin (keV)	Counts	Fraction	dE/dx (keV/um)	En.loss (keV) (in 2.3 um Au)			
0-500	39550	21.2%	206	250	(range p@525 keV = 2.3 um)		
500-1000	37650	20.2%	140.1	322			
1000-1500	1560	0.8%	111	255			
1500-2000	75550	40.5%	95.1	219			
2000-2500	32150	17.2%	83.8	193			
2500-3000	0	0.0%	75.3	173			

Table 6.1.1.2: P+ backscatter ratio in a typical Aerosol measurement scenario

Following these simulations the protons giving worse effects are those releasing energy below 300 keV in the absorber, in this view possible countermeasures (like e.g. a deflector) could be limited to work effectively on protons up to 1 MeV possibly easing e.g. the High-Voltage constraints in case of an electrostatic deflector.

6.1.2 Main effects on pixels and detector bulk

We expect two different effects from protons impinging on the detector chip:

a) Proton hitting a pixel releasing energy in the 2.3 µm gold absorber
b) Proton hitting the bulk of the chip releasing energy in the 300 µm silicon substrate

The effect on the pixel will be a temporary blinding of the chip due to the high energy release causing saturation, this is accounted as dead time of the pixel.

The effect on the bulk silicon will be a random perturbation in the thermal balance of the system leading to a loss of resolution.

To estimate the disturbances caused by this effect we could scale from a few available X-IFU measurements and simulations.

OPEN

6.1.3 Effects on dead time

For what concern the pixel dead time we can rely on measurements on a similar prototype pixels showing a pulse duration of ~ 6.5 ms for an energy release of 50 keV.
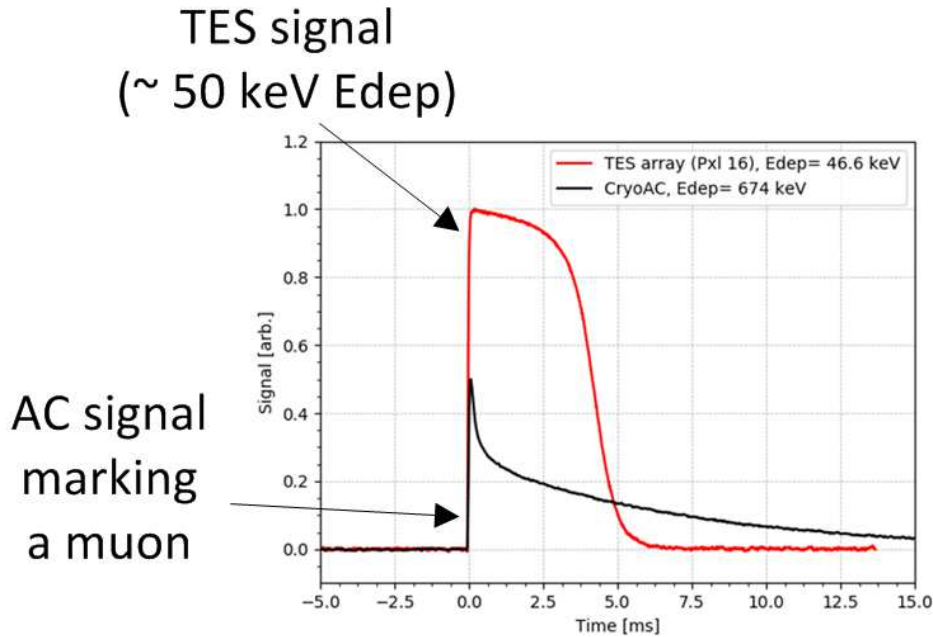

Fig. 6.1.3.1: excerpt from the CryoAC DM test data [ref. RD12]

At the same time we expect that the maximum energy release (non-MIP particle) in the 2.3 µm gold absorber is in the order of 300 keV.
Taking a rough linear estimate we get a maximum dead time after a P+ hit of ~ 40 ms.

Dead time caused by protons hits (assume 40 ms / proton hit):

2 % to 10 % (cultural heritage)

16 % to 80 % (aerosol)

From this preliminary evaluation we understand that the Aerosol scenario is critical for set up with count rate above the minimum.

OPEN

6.1.4 Effects on energy resolution

For what concern the loss of resolution due to interactions in the bulk we can scale from a set of simulations showing that Cosmic Rays (MIP) releasing ~ 0.15 MeV in the 300 µm Si bulk with a rate of 200 cps cause a loss of resolution of 0.06 eV.
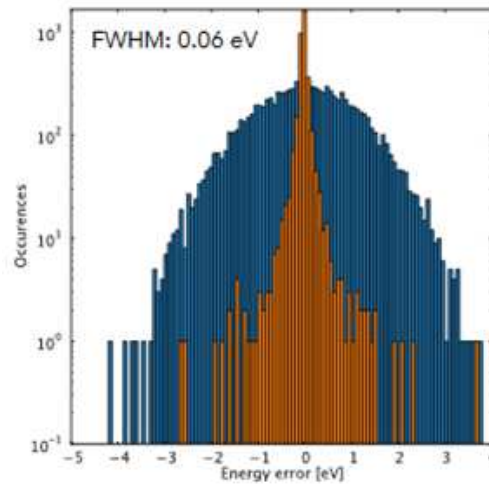

Fig. 6.1.4.1: Excerpt from the CryoAC simulation [ref. RD11]

For non-MIP particles we expect a maximum release of 3 MeV in the bulk and scaling for the maximum rate of 500 cps (worst case Aerosol campaign, 1 P+ every 10 photons) we can roughly estimate a loss of resolution of:

$$0.06 \ [eV] \cdot (500 \ [cps] \ / \ 200 \ [cps]) \cdot (3 \ [MeV] \ / \ 0.15 \ [MeV]) \sim 3 \ eV$$

6.2   Mitigation of the backscattered protons effects

Following the evaluations described in the preceding chapter it is envisaged a study of mitigation action to counteract the effect of backscattered protons.
These countermeasures are to be applied acting externally from the cryostat/probe assembly to avoid additional burden on the design activities. The baseline is to use a set-up (geometry, collimators beam intensity etc.) optimized to minimize the P+ backscattering and to install a sort of P+ deflector in the space between the target and the probe entrance window.

The standard way to tackle the backscattering is to place a strong magnet close to the target to deflect the protons. In this case the use of a deflector magnet is not preferred due to presence of B-sensitive devices (TES, SQUID) and a research effort is envisaged to use some electrostatic deflectors instead (possibly Einzel lens used as divertors).

OPEN
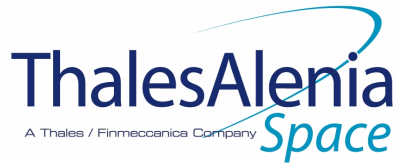
The Electrostatic deflector is presently the baseline approach.
A magnetic deflector is still kept as a backup solution in view of the possible difficulties with setting HV plates in the crumped space between target and entrance window.
In this case we will need special designed magnets with very thin gap to reduce stray fields.
As a last resource we may limit the proton beam energy to 2 MeV and interpose a thin absorber (e.g. few tens of μm Mylar) to stop the backscattered protons at the expense of a cut in the lower energy spectrum.

7. ANNEX2 POSSIBLE IMPROVEMENTS FOR AN UPDATED DESIGN

We reports here a few possible improvements which are not included in the present design baseline but could be implemented in a future revision after having verified the overall performances of the instrument.

A tapered front side of the snout could improve the FOV by a factor 1.5 or 2, this would require a redesign of the front caps at each stage and possibly a minor redesign of the detector holder volume.

An external window, and internal filters, based on aluminized silicon nitride could be adopted to optimize the QE of the system at low energies (< 2 keV).

END OF DOCUMENT

OPEN

Template 83230326-DOC-TAS-EN/003